J. Plasma Phys. (2018), *vol.* 84, 775840603
doi:10.1017/S0022377818001228

Mass and internal-energy transports in strongly compressible magnetohydrodynamic turbulence

N. Yokoi[1,2,†]

[1]Institute of Industrial Science, University of Tokyo, 4-6-1, Komaba, Tokyo 153-8505, Japan

[2]Nordic Institute for Theoretical Physics (NORDITA), Roslagstullsbacken 23, 106 91 Stockholm, Sweden

(Received 8 August 2018; revised 7 November 2018; accepted 8 November 2018)

Turbulent mass and internal-energy transports in strongly compressible magnetohydrodynamic (MHD) turbulence are investigated in the framework of the multiple-scale direct-interaction approximation, an analytical closure scheme for inhomogeneous turbulence at very high Reynolds numbers. Utilising the analytical representations for the turbulent mass and internal-energy fluxes and their transport coefficients, which are expressed in terms of the correlation and response functions, turbulence models for these fluxes are proposed. In addition to the usual gradient-diffusion transports, cross-diffusion transports mediated by the density variance and the transports along the mean magnetic field mediated by the compressional or dilatational turbulent cross-helicity (velocity–magnetic-field correlation coupled with compressive motions) are shown to arise. These compressibility effects are of fundamental importance since they provide deviations from the usual gradient-diffusion transports. Analogies of the dilatational cross-helicity effects to the magnetoacoustic waves are also argued.

Key words: astrophysical plasmas, plasma nonlinear phenomena, plasma waves

1. Introduction

Material flows and energy transfers arise as a result of non-uniform spatial distributions of fluid material, energy, flow velocity, etc. in several forms of physical processes such as diffusion, convection, conduction, radiation, etc. For large-scale structures and their evolutions of mass density and internal energy or heat, turbulent motions are considered to play essential roles in determining the effective transports of the mass and internal energy. The turbulent mass flux $\langle \rho' \boldsymbol{u}' \rangle$ and internal-energy flux $\langle q' \boldsymbol{u}' \rangle$ are the most important turbulent correlations which determine the spatio-temporal evolutions of the mean density $\overline{\rho}$ and the mean internal energy Q (ρ': density fluctuation, $\boldsymbol{u}'$: velocity fluctuation, q': internal-energy fluctuation, $\langle \cdots \rangle$: ensemble average). In real-world turbulent flows at very large Reynolds numbers, the turbulent mass and internal-energy fluxes are so dominant that proper evaluation and modelling of $\langle \rho' \boldsymbol{u}' \rangle$ and $\langle q' \boldsymbol{u}' \rangle$ are of crucial importance.

† Email address for correspondence: nobyokoi@iis.u-tokyo.ac.jp

There are several levels of modelling of the mass and internal-energy fluxes. In the simplest case, the turbulent fluxes are modelled using an algebraic gradient-diffusion approximation with a prescribed distribution of the mixing length for expressing the eddy diffusivities. The gradient-diffusion approximations of the turbulent mass and internal-energy fluxes, $\langle \rho' \boldsymbol{u}' \rangle = -\kappa_{\mathrm{T}} \nabla \overline{\rho}$ and $\langle q' \boldsymbol{u}' \rangle = -\eta_{\mathrm{T}} \nabla Q$, respectively, are most widely used in the engineering, geophysical and astrophysical fields (Tennekes & Lumley 1972; Turner 1973; Kaviany 2001; Kupka 2009). However, it is well recognised that the gradient diffusion is not necessarily the best approximation for the turbulent transport: the so-called 'gradient-transport fallacy' (Tennekes & Lumley 1972). Firstly, the transport coefficient is not dynamically derived but obtained just by a dimensional analysis as in the mixing-length theory. Secondly, the gradient-transport model assumes the locality of the turbulent transport in space and time. In the real-world turbulence, non-locality in space and time often plays an important role in determining the effective transport. In particular, in the convective turbulence at high Rayleigh numbers, implementation of the non-local effects due to plumes and thermals is known to be very important. How to incorporate the turbulent entrainment effects into the modelling of the turbulent mass and heat fluxes is one of the central issues in convective turbulence (Linden 2000; Kaviany 2001). Thirdly, in general, in the presence of some breakage of symmetry in turbulence, not only transport enhancement but also transport suppression due to turbulence shows up. This is typically the case in dynamos, where the turbulent magnetic diffusivity (a gradient diffusion) can be counter-balanced by some other effects represented by the field-generation mechanisms such as the α effect (Parker 1955; Moffatt 1978; Krause & Rädler 1980), also the case in turbulent magnetic reconnections, as has been recently pointed out (Higashimori, Yokoi & Hoshino 2013; Yokoi, Higashimori & Hoshino 2013; Widmer, Büchner & Yokoi 2016*a*,*b*). Such a transport suppression mechanism is also investigated in hydrodynamic turbulence in the context of the helicity effect in global flow generation (Yokoi & Yoshizawa 1993; Yokoi & Brandenburg 2016).

In astrophysical flow phenomena, turbulence is considered to play a key role in determining the effective material and energy transports. One of the most important topics related to strongly compressible MHD turbulence is star formation. In order to understand the dynamic properties of galaxies, it is required to understand how, where and under which conditions stars form. It is considered that the star formation rate is controlled by molecular cloud formation and support by supersonic turbulence in the interplay with gravity (Mac Low & Klessen 2004; McKee & Ostriker 2007). For the recent developments of numerical studies of the interstellar turbulence, including comparisons with theories and observations, the reader is referred to, for example, elaborate works by Federrath & Klessen (2012) and Kritsuk, Ustyugov & Norman (2017) and works cited therein.

In the usual turbulence simulation studies with a periodic box, the effects of turbulence on the star formation rate are often argued in the context of the dependence on the amount of compression induced by the turbulence forcing mechanism, the global sonic Mach number, the degree of magnetisation represented by the externally imposed magnetic field and/or the Alfvén Mach number, etc. At the same time, in order to treat the dynamic behaviour of star formation, it is desirable to understand how and how much turbulent transport we have in realistic astrophysical parameters. In the framework of inhomogeneous turbulence or turbulence modelling with non-uniform mean fields, the transports of the material, momentum, energy, etc. due to turbulence are represented by turbulence correlations such as the turbulent mass flux, the Reynolds and turbulent Maxwell stresses, the turbulent energy flux, etc.

https://doi.org/10.1017/S0022377818001228 Published online by Cambridge University Press

The dynamic properties of the star formation rate should be argued in terms of how the turbulent transport coefficients coupled with the mean-field inhomogeneities are determined by the compressible properties of the magnetised turbulence. In this sense, test or validation of the model expressions in realistic star formation situations would be of primary importance.

Another important astrophysical application of the compressible MHD turbulence is the core collapse supernova (CCSN) explosion problem: to understand how the stalled shock transitions into a dynamic explosion. It has been recently recognised that turbulence enables the CCSN explosion. How to model turbulence effects in neutrino heating is one of the central issues for understanding the explosion condition (Mabanta & Murphy 2018). Several types of turbulence models have been examined in comparison with two-dimensional numerical simulations. It is shown that the usual local gradient-diffusion transport models of the turbulent energy flux are inappropriate, as has been demonstrated in comparison with a series of three-dimensional simulations of the turbulent stellar interiors (Meakin & Arnett 2010). Instead, a global balance model representing the coherent plume effects gives much more reasonable results (Murphy & Meakin 2011).

As the turbulence modelling in the CCSN explosion shows as an example, a turbulence model just based on the simple local gradient transport, which represents the primary local transport effect, is not sufficient in many cases. At least we need some deviations from the gradient-diffusion models. In order to get a proper model, heuristic arguments are not necessarily enough. Rather, we should start from the fundamental equations, and derive more generic expressions for the turbulence correlations relevant to the mean-field equations.

The multiple-scale direct-interaction approximation (multiple-scale DIA) is an analytical closure scheme which treats inhomogeneous turbulence with non-uniform mean fields at very high Reynolds numbers (Yoshizawa 1984) (also for applications to magnetohydrodynamic (MHD) turbulence, see Yoshizawa 1990; Yoshizawa & Yokoi 1993; Yokoi 2013). This theoretical formulation is suitable for a systematic derivation of the analytical expressions of the turbulent correlations in strongly nonlinear and inhomogeneous systems. As compared with the previous multiple-scale attempt in compressible MHD turbulence analysis with a Markovianised approximation in the configuration space (Yoshizawa 1996), the present approach requires highly elaborate calculations. At the cost of such lengthy analytical calculations, we obtain more precise expressions since we use more accurate treatments based on exact mathematical relationships in wavenumber space. In this paper, with the aid of this multiple-scale DIA scheme, we investigate a full system of equations for strongly compressible MHD turbulence. In a recent paper (Yokoi 2018) (hereafter denoted as Paper 1), special emphasis was placed on the turbulent electromotive force $\langle \boldsymbol{u}' \times \boldsymbol{b}' \rangle$ in the mean magnetic induction equation. Here in this work, we focus our attention on the turbulent mass flux $\langle \rho' \boldsymbol{u}' \rangle$ and the turbulent internal-energy flux $\langle q' \boldsymbol{u}' \rangle$.

The organisation of this paper is as follows. In § 2, the fundamental MHD equations and the turbulent correlations relevant to the mean-field evolutions are presented. In § 3, the procedure of the multiple-scale direct-interaction approximation is briefly shown. In § 4, the analytical expressions of the turbulent mass and internal-energy fluxes are derived, and turbulence modelling on the basis of the theoretical results is presented. In § 5, physical interpretations of the effects causing the deviations from the gradient-diffusion transports are presented, followed by the comparison with the linear MHD-wave effects. Concluding remarks including notes on the source of the compressional turbulent cross-helicity are given in § 6.

https://doi.org/10.1017/S0022377818001228 Published online by Cambridge University Press

2. Turbulent correlations

2.1. *Fundamental equations*

The equations of the density ρ, the velocity $\boldsymbol{u}$, the internal energy q and the magnetic field $\boldsymbol{b}$ are given by

$$\frac{\partial \rho}{\partial t} + \nabla \cdot (\rho \boldsymbol{u}) = 0, \tag{2.1}$$

$$\frac{\partial}{\partial t}\rho u^\alpha + \frac{\partial}{\partial x^a}\rho u^a u^\alpha = -\frac{\partial p}{\partial x^\alpha} + \frac{\partial}{\partial x^a}\mu s^{a\alpha} + \frac{1}{\mu_0}(\boldsymbol{j}\times\boldsymbol{b})^\alpha + f_{\mathrm{ex}}^\alpha, \tag{2.2}$$

$$\frac{\partial}{\partial t}\rho q + \nabla \cdot (\rho \boldsymbol{u} q) = \nabla \cdot (\kappa \nabla \theta) - p \nabla \cdot \boldsymbol{u} + \phi, \tag{2.3}$$

$$\frac{\partial \boldsymbol{b}}{\partial t} = -\nabla \times \boldsymbol{e}, \tag{2.4}$$

with Ohm's law for moving media:

$$\boldsymbol{j} = \frac{1}{\mu_0}\nabla \times \boldsymbol{b} = \sigma(\boldsymbol{e} + \boldsymbol{u}\times\boldsymbol{b}), \tag{2.5}$$

where p is the plasma gas pressure, μ the viscosity, $\boldsymbol{j}$ the electric-current density, $\boldsymbol{e}$ the electric field, κ the thermal conductivity, μ_0 the magnetic permeability, σ the electric conductivity and $s^{\alpha\beta}$ the deviatoric or traceless part of the velocity strain defined by

$$s^{\alpha\beta} = \frac{\partial u^\beta}{\partial x^\alpha} + \frac{\partial u^\alpha}{\partial x^\beta} - \frac{2}{3}\nabla \cdot \boldsymbol{u}\delta^{\alpha\beta}. \tag{2.6}$$

In (2.2), $\boldsymbol{f}_{\mathrm{ex}}$ represents the external forces including the gravity force and external forcing. In what follows, we pay more attention to the theoretical formulation of the nonlinear turbulence dynamics that does not directly depend on specific forcing effects, so we neglect $\boldsymbol{f}_{\mathrm{ex}}$ hereafter. In (2.3) ϕ is the dissipation function that represents the conversion of kinetic and magnetic energies to heat through the molecular effects:

$$\phi = \mu s^{ab}\frac{\partial u^a}{\partial x^b} + \frac{1}{\sigma}\boldsymbol{j}^2. \tag{2.7}$$

In the following theoretical calculations, ϕ is also neglected since our main interests lie in the p-related effects in the turbulent transport. Note that these treatments do not deny the importance of the external forces and the dissipation function. Actually, in order to sustain turbulence and its evolution properties, including energies and helicities, those effects play important roles.

The pressure p is related to the temperature θ and the internal energy q as

$$p = R\rho\theta = (\gamma_{\mathrm{s}} - 1)\rho q, \tag{2.8}$$

where

$$q = C_V(\theta)\theta. \tag{2.9}$$

Here, C_V is the specific heat at constant volume, R is the gas constant and γ_{s} is the ratio of C_P (the specific heat at constant pressure) to C_V.

https://doi.org/10.1017/S0022377818001228 Published online by Cambridge University Press

From (2.4) and (2.5), the induction equation of the magnetic field is written as

$$\frac{\partial \boldsymbol{b}}{\partial t} = \boldsymbol{\nabla} \times (\boldsymbol{u} \times \boldsymbol{b}) + \eta \nabla^2 \boldsymbol{b} \tag{2.10}$$

or

$$\frac{\partial \boldsymbol{b}}{\partial t} + (\boldsymbol{u} \cdot \boldsymbol{\nabla})\boldsymbol{b} = (\boldsymbol{b} \cdot \boldsymbol{\nabla})\boldsymbol{u} - \boldsymbol{b}\boldsymbol{\nabla} \cdot \boldsymbol{u} + \eta \nabla^2 \boldsymbol{b}, \tag{2.11}$$

where η is the magnetic diffusivity defined as $\eta = 1/(\sigma \mu_0)$.

2.2. *Mean-field equations*

In contrast to the constant density cases, the physical interpretation of the mean-field transport expressions is not unique when the density varies. Due to the additional correlations originating from the variable density, the system of the mean-field transport equations is much more complicated. The structure and the meaning of the transport expression; which turbulence correlations appear and what is their physical interpretation, depend on the averaging formulation. If we adopt mass-weighted averaging, the density-fluctuation correlations can be formally removed from the mean transport expressions. This allows the variable density case to be treated in a strong analogy with the constant density case. Because of this property, mass-weighted averaging is often adopted in compressible turbulence studies. As an example of the recent works with mass-weighted decomposition, Aluie (2011) applied this formulation to the energy transfer function of compressible turbulence, and argued that the cascade of the mean kinetic energy occurs in a conservative and scale-local manner due to the statistical decoupling between the mean kinetic and internal-energy budgets.

Although all the different averaging formulations are algebraically equivalent to each other, their physical interpretations of the turbulence correlations can be entirely different. As for detailed descriptions on the statistical averaging in variable density fluid turbulent motion, the reader is referred to chapter 5 of Chassaing *et al.* (2002), which includes the formal mathematical relationship and physical comparison between the mass-weighted and Reynolds averaging.

In the mass-weighted averaging formulation, all the density-fluctuation correlations are implicitly embedded in the mean values. This makes it very difficult to identify all the density-fluctuation correlation effects. In order to see the explicit effects of the density fluctuation in the mass and internal-energy equations, we adopt ensemble or Reynolds averaging in this work.

With the Reynolds averaging denoted by $\langle \cdots \rangle$, a field quantity f is divided into the mean F and the fluctuation around it, f', as

$$f = F + f', \quad F = \langle f \rangle, \tag{2.12}$$

with

$$f = (\rho, \boldsymbol{u}, q, \theta, \boldsymbol{b}, \boldsymbol{j}, \boldsymbol{e}), \tag{2.13a}$$

$$F = (\overline{\rho}, \boldsymbol{U}, Q, \Theta, \boldsymbol{B}, \boldsymbol{J}, \boldsymbol{E}), \tag{2.13b}$$

$$f' = (\rho', \boldsymbol{u}', q', \theta', \boldsymbol{b}', \boldsymbol{j}', \boldsymbol{e}'). \tag{2.13c}$$

With the Reynolds decomposition (2.12), the mean density equation is given by

$$\frac{\partial \overline{\rho}}{\partial t} + \boldsymbol{\nabla} \cdot (\overline{\rho} \boldsymbol{U}) = -\boldsymbol{\nabla} \cdot \langle \rho' \boldsymbol{u}' \rangle. \tag{2.14}$$

https://doi.org/10.1017/S0022377818001228 Published online by Cambridge University Press

The mean velocity equation is written as

$$\frac{\partial}{\partial t}\overline{\rho}U^{\alpha}+\frac{\partial}{\partial x^{a}}\overline{\rho}U^{a}U^{\alpha}=-(\gamma_{s}-1)\frac{\partial}{\partial x^{\alpha}}\overline{\rho}Q+\frac{\partial}{\partial x^{\alpha}}\overline{\mu}\mathcal{S}^{a\alpha}+(\boldsymbol{J}\times\boldsymbol{B})^{\alpha}$$
$$-\frac{\partial}{\partial x^{\alpha}}\left(\overline{\rho}\langle u'^{a}u'^{\alpha}\rangle-\frac{1}{\mu_{0}}\langle b'^{a}b'^{\alpha}\rangle+U^{a}\langle\rho'u'^{\alpha}\rangle+U^{\alpha}\langle\rho'u'^{a}\rangle\right)+R_{U}^{\alpha}, \tag{2.15}$$

where $\overline{\mu}$ is the mean part of the viscosity and $\boldsymbol{S}=\{\mathcal{S}^{\alpha\beta}\}$ is the deviatoric or traceless part of the mean velocity strain tensor defined by

$$\mathcal{S}^{\alpha\beta}=\frac{\partial U^{\beta}}{\partial x^{\alpha}}+\frac{\partial U^{\alpha}}{\partial x^{\beta}}-\frac{2}{3}\nabla\cdot\boldsymbol{U}\delta^{\alpha\beta}. \tag{2.16}$$

The mean internal-energy equation is written as

$$\frac{\partial}{\partial t}\overline{\rho}Q+\nabla\cdot(\overline{\rho}\boldsymbol{U}Q)=\nabla\cdot\left(\frac{\overline{\kappa}}{C_{V}}\nabla Q\right)-\nabla\cdot(\overline{\rho}\langle q'\boldsymbol{u}'\rangle+Q\langle\rho'\boldsymbol{u}'\rangle+\boldsymbol{U}\langle\rho'q'\rangle)$$
$$-(\gamma_{s}-1)(\overline{\rho}Q\nabla\cdot\boldsymbol{U}+\overline{\rho}\langle q'\nabla\cdot\boldsymbol{u}'\rangle+Q\langle\rho'\nabla\cdot\boldsymbol{u}'\rangle)+R_{Q}, \tag{2.17}$$

where $\overline{\kappa}$ is the mean part of the diffusivity. And the mean magnetic induction equation is written as

$$\frac{\partial\boldsymbol{B}}{\partial t}=\nabla\times(\boldsymbol{U}\times\boldsymbol{B}+\langle\boldsymbol{u}'\times\boldsymbol{b}'\rangle)+\eta\nabla^{2}\boldsymbol{B}. \tag{2.18}$$

In (2.15) and (2.17), $\boldsymbol{R}_{U}$ and R_{Q} are the terms expected to be small, whose detailed expressions are suppressed here.

In the mean-field equations (2.14), (2.15), (2.17) and (2.18), we have the turbulent mass flux $\langle\rho'\boldsymbol{u}'\rangle$, the Reynolds stress $\langle\boldsymbol{u}'\boldsymbol{u}'\rangle$, the turbulent Maxwell stress $\langle\boldsymbol{b}'\boldsymbol{b}'\rangle$, the turbulent heat flux $\langle q'\boldsymbol{u}'\rangle$, the turbulent electromotive force $\langle\boldsymbol{u}'\times\boldsymbol{b}'\rangle$, etc. These turbulence correlations represent the turbulence effects and play key roles in determining the effective transports due to turbulence. The evaluation of these turbulent correlations is the central objective of this work.

2.3. *Fluctuation equations*

Subtracting the mean-field equations (2.14), (2.15), (2.17) and (2.18) from the fundamental equations (2.1)–(2.3) and (2.11), we obtain the equations of the fluctuations as

$$\frac{\mathrm{D}\rho'}{\mathrm{D}t}+\nabla\cdot(\rho'\boldsymbol{u}')+\overline{\rho}\nabla\cdot\boldsymbol{u}'=-(\boldsymbol{u}'\cdot\nabla)\overline{\rho}-\rho'\nabla\cdot\boldsymbol{U}+\nabla\cdot\langle\rho'\boldsymbol{u}'\rangle, \tag{2.19}$$

$$\frac{\mathrm{D}u'^{\alpha}}{\mathrm{D}t}=-(\boldsymbol{u}'\cdot\nabla)u'^{\alpha}+\frac{1}{\overline{\rho}}\frac{\partial}{\partial x^{a}}\overline{\mu}s'^{a\alpha}-(\gamma_{\mathrm{s}}-1)\left(\frac{\partial q'}{\partial x^{\alpha}}+\frac{Q}{\overline{\rho}}\frac{\partial\rho'}{\partial x^{\alpha}}\right)$$
$$+\frac{1}{\mu_{0}\overline{\rho}}[(\boldsymbol{b}'\cdot\nabla)b'^{\alpha}+(\boldsymbol{B}\cdot\nabla)b'^{\alpha}]-(\boldsymbol{u}'\cdot\nabla)U^{\alpha}-(\gamma_{\mathrm{s}}-1)\left(\frac{\rho'}{\overline{\rho}}\frac{\partial Q}{\partial x^{\alpha}}+\frac{q'}{\overline{\rho}}\frac{\partial\overline{\rho}}{\partial x^{\alpha}}\right)$$
$$+\frac{1}{\mu_{0}\overline{\rho}}(\boldsymbol{b}'\cdot\nabla)B^{\alpha}-\frac{\rho'}{\overline{\rho}}\frac{\mathrm{D}U^{\alpha}}{\mathrm{D}t}+R_{u}^{\alpha}, \tag{2.20}$$

https://doi.org/10.1017/S0022377818001228 Published online by Cambridge University Press

$$\frac{\mathrm{D}q'}{\mathrm{D}t} + (\boldsymbol{u}'\cdot\nabla)q' - \frac{1}{\overline{\rho}}\nabla\cdot\left(\frac{\overline{\kappa}}{C_V}\nabla q'\right) + (\gamma_\mathrm{s}-1)Q\nabla\cdot\boldsymbol{u}' = -(\boldsymbol{u}'\cdot\nabla)Q - (\gamma_\mathrm{s}-1)\left(q' + \frac{\rho'}{\overline{\rho}}Q\right)\nabla\cdot\boldsymbol{U}, \tag{2.21}$$

$$\frac{\mathrm{D}\boldsymbol{b}'}{\mathrm{D}t} + (\boldsymbol{u}'\cdot\nabla)\boldsymbol{b}' - (\boldsymbol{b}'\cdot\nabla)\boldsymbol{u}' - \eta\nabla^2\boldsymbol{b}' - (\boldsymbol{B}\cdot\nabla)\boldsymbol{u}' + \boldsymbol{B}\nabla\cdot\boldsymbol{u}' = -(\boldsymbol{u}'\cdot\nabla)\boldsymbol{B} + (\boldsymbol{b}'\cdot\nabla)\boldsymbol{U} - \boldsymbol{b}'\nabla\cdot\boldsymbol{U} + R_b^\alpha, \tag{2.22}$$

where $\mathrm{D}/\mathrm{D}t(=\partial/\partial t + \boldsymbol{U}\cdot\nabla)$ is the mean-flow convective derivative, and $\boldsymbol{R}_u$ and $\boldsymbol{R}_b$ are the higher-order terms whose detailed expressions are suppressed here.

If the fluctuations or perturbations are small, the nonlinear products of them can be neglected in the evolution of the fluctuation fields. This quasi-linearity is often the starting point of the linear wave and instability studies. However, this is not the case for fully developed turbulent flows with astrophysical and geophysical interests. In realistic turbulent flows with large kinetic and magnetic Reynolds numbers, the nonlinear coupling terms, such as $\nabla\cdot(\rho'\boldsymbol{u}')$ in (2.19), $(\boldsymbol{u}'\cdot\nabla)\boldsymbol{u}'$ and $(\boldsymbol{b}'\cdot\nabla)\boldsymbol{b}'$ in (2.20), $(\boldsymbol{u}'\cdot\nabla)q'$ in (2.21), $(\boldsymbol{u}'\cdot\nabla)\boldsymbol{b}'$ and $(\boldsymbol{b}'\cdot\nabla)\boldsymbol{u}'$ in (2.22), etc., are not small and cannot be neglected at all. Here, we have to simultaneously treat the effects of strong nonlinearity and inhomogeneity. In the following section, we present a framework of how to address such nonlinear and inhomogeneous turbulent flows.

3. Multiple-scale analysis

In order to evaluate the turbulent correlations, we analyse the equations of the fluctuation density ρ' (2.19), fluctuation velocity $\boldsymbol{u}'$ (2.20), fluctuation internal energy q' (2.21) and fluctuation magnetic field $\boldsymbol{b}'$ (2.22) in the framework of the multiple-scale direct-interaction approximation. This is a closure scheme for inhomogeneous turbulence at very high Reynolds numbers (Yoshizawa 1984).

The formal procedure of the multiple-scale analysis is constituted by:

(i) introduction of multiple scales;
(ii) Fourier representation with respect to the fast variable;
(iii) scale-parameter expansion;
(iv) basic-field expansion and introduction of the Green's functions;
(v) statistical assumption on the lowest-order fields;
(vi) calculation of the correlations with renormalisation.

Since application of this scheme to fully compressible magnetohydrodynamic (MHD) turbulence was already presented in our recent paper (Yokoi 2018) (Paper 1), here we do not show the details of each stage, but show the basic idea of the formulation. As for the detailed procedure of the approximation, the reader is referred to Paper 1. Also on the basic assumptions and approximations of the scheme, see Yokoi (2013).

(i) Introduction of multiple scales

We introduce two scales by the fast and slow variables as

$$\boldsymbol{\xi} = \boldsymbol{x}, \quad \boldsymbol{X} = \delta\boldsymbol{x}; \quad \tau = t, \quad T = \delta t. \tag{3.1a–d}$$

If δ is small, the variations of $\boldsymbol{X}$ and T are not negligible only when the original variables $\boldsymbol{x}$ and t change considerably. In this sense, $\boldsymbol{X}$ and T are suitable for

https://doi.org/10.1017/S0022377818001228 Published online by Cambridge University Press

describing the slow variations, and are called the slow variables, while $\boldsymbol{\xi}$ and τ are fast variables. With these variables, a field quantity f is assumed to be decomposed into

$$f = F(\boldsymbol{X}; T) + f'(\boldsymbol{\xi}, \boldsymbol{X}; \tau, T). \tag{3.2}$$

Under (3.1), the spatial and time partial derivatives are written as

$$\nabla_x = \nabla_\xi + \delta \nabla_X, \quad \frac{\partial}{\partial t} = \frac{\partial}{\partial \tau} + \delta \frac{\partial}{\partial T}. \tag{3.3a,b}$$

This is a derivative expansion: the derivatives with respect to the slow variables, ∇_X and $\partial/\partial T$, show up with δ. We apply this multiple-scale procedure with (3.1)–(3.3) to the fundamental equations.

(ii) Fourier representation with respect to the fast variable

We use the Fourier representation with respect to the fast spatial variable $\boldsymbol{\xi}$ as

$$f'(\boldsymbol{\xi}, \boldsymbol{X}; \tau, T) = \frac{1}{(2\pi)^3} \int \mathrm{d}\boldsymbol{k} \hat{f}'(\boldsymbol{k}, \boldsymbol{X}; \tau, T) \exp[-\mathrm{i}\boldsymbol{k} \cdot (\boldsymbol{\xi} - \boldsymbol{U}\tau)]. \tag{3.4}$$

The factor $\mathrm{i}\boldsymbol{k} \cdot (\boldsymbol{\xi} - \boldsymbol{U}\tau)$ means that the fast-varying turbulence is treated in the frame moving with the velocity $\boldsymbol{U}$. Hereafter, the hat for the Fourier component $\hat{f}$ is dropped.

(iii) Scale-parameter expansion

Then, the fluctuation fields are expanded with respect to a scale parameter δ:

$$f' = \sum_{n=0}^{\infty} \delta^n f'_n. \tag{3.5}$$

Note that the scale parameter δ is associated with the large-scale inhomogeneities as in (3.3). The lowest-order field is homogeneous, and the mean-field inhomogeneity effects are taken into account through the higher-order terms in δ.

(iv) Basic-field expansion and introduction of the Green's functions

In the framework of the multiple-scale DIA, the system of equations of the fluctuation fields $f' = (\rho', \boldsymbol{u}', q', \boldsymbol{b}')$ is formally solved with the aid of the Green's functions associated with the lowest-order fields $f'_0 = (\rho'_0, \boldsymbol{u}'_0, q'_0, \boldsymbol{b}'_0)$. These Green's functions G'_ρ, G'_u, G'_q and G'_b are nonlinearly coupled to each other. Actually, even in the solenoidal case without the density or internal-energy fluctuations, we have to introduce at least four Green's functions for the velocity and magnetic-field fluctuations: G'_{uu} for the velocity response to the velocity, G'_{ub} for the velocity response to the magnetic field, G'_{bu} for the magnetic-field response to the velocity, G'_{bb} for the magnetic-field response to the magnetic field. This situation is too much complicated. In order to reduce this complexity, we introduce the basic fields. The lowest-order fields $f'_0 = (\rho'_0, \boldsymbol{u}'_0, q'_0, \boldsymbol{b}'_0)$ are expanded as

$$f'_0 = f'_{\mathrm{B}} + \sum_{m=1}^{\infty} f'_{0m}, \tag{3.6}$$

where m is the number of iterations. The system of lowest-order field equations is solved in an iterative manner.

https://doi.org/10.1017/S0022377818001228 Published online by Cambridge University Press

Here we should note the following point on the solenoidal property of each order of the field quantities. In the present multiple-scale formulation with (3.3), the divergence of a fluctuating vector field is written as

$$\nabla \cdot \boldsymbol{f}'(\boldsymbol{x}; t) = \frac{\partial f'^a(\boldsymbol{\xi}, \boldsymbol{X}; \tau, T)}{\partial \xi^a} + \delta \frac{\partial f'^a(\boldsymbol{\xi}, \boldsymbol{X}; \tau, T)}{\partial X^a}, \tag{3.7}$$

or equivalently in the wavenumber space as

$$\nabla \cdot \boldsymbol{f}'(\boldsymbol{k}, \boldsymbol{X}; \tau, T) = -\mathrm{i}k^a f'^a(\boldsymbol{k}, \boldsymbol{X}; \tau, T) + \delta \frac{\partial f'^a(\boldsymbol{k}, \boldsymbol{X}; \tau, T)}{\partial X_{\mathrm{I}}^a}, \tag{3.8}$$

where

$$\frac{\partial}{\partial X_{\mathrm{I}}^a} = \exp(-\mathrm{i}\boldsymbol{k} \cdot \boldsymbol{U}\tau) \frac{\partial}{\partial X^a} \exp(\mathrm{i}\boldsymbol{k} \cdot \boldsymbol{U}\tau) \tag{3.9}$$

is the so-called interaction representation of the spatial derivative associated with (3.4). In order to secure the divergence-free condition for the solenoidal or incompressible field quantities, we introduce the solenoidal field $\boldsymbol{f}'_{\mathrm{S}}(\boldsymbol{k}, \boldsymbol{X}; \tau, T)$ as

$$f'^{\,\alpha}_{\mathrm{S}}(\boldsymbol{k}, \boldsymbol{X}; \tau, T) = f'^{\alpha}(\boldsymbol{k}, \boldsymbol{X}; \tau, T) + \delta \frac{k^\alpha}{k^2} \frac{\partial f'^a(\boldsymbol{k}, \boldsymbol{X}; \tau, T)}{\partial X_{\mathrm{I}}^a}, \tag{3.10}$$

which satisfies the solenoidal condition as

$$k^a f'^{\,a}_{\mathrm{S}}(\boldsymbol{k}, \boldsymbol{X}; \tau, T) = k^a f'^a(\boldsymbol{k}, \boldsymbol{X}; \tau, T) + \delta \frac{k^a k^a}{k^2} \frac{\partial f'^b(\boldsymbol{k}, \boldsymbol{X}; \tau, T)}{\partial X_{\mathrm{I}}^b} = 0 \tag{3.11}$$

in the wavenumber space (Hamba 1987).

We introduce the Green's functions of the basic fields, which are uncoupled with each other, as

$$\frac{\partial G'_\rho(\boldsymbol{k}; \tau, \tau')}{\partial \tau} - \mathrm{i}k^a \iint \delta(\boldsymbol{k} - \boldsymbol{p} - \boldsymbol{q})\, \mathrm{d}\boldsymbol{p}\, \mathrm{d}\boldsymbol{q} u'^{\,a}_{\mathrm{B}}(\boldsymbol{p}; \tau) G'_\rho(\boldsymbol{q}; \tau, \tau') = \delta(\tau - \tau'), \tag{3.12}$$

$$\frac{\partial G'^{\,\alpha a}_u(\boldsymbol{k}; \tau, \tau')}{\partial \tau} + \bar{\nu} k^2 G'^{\,\alpha a}_u(\boldsymbol{k}; \tau, \tau') + \frac{1}{3} \bar{\nu} k^\alpha k^b G'^{\,ba}_u(\boldsymbol{k}; \tau, \tau')$$
$$- 2\mathrm{i} \iint \delta(\boldsymbol{k} - \boldsymbol{p} - \boldsymbol{q})\, \mathrm{d}\boldsymbol{p}\, \mathrm{d}\boldsymbol{q} M_{\mathrm{c}}^{\alpha bc} u'^{\,b}_{\mathrm{B}}(\boldsymbol{p}; \tau) G'^{\,ca}_u(\boldsymbol{q}; \tau, \tau') = \delta^{\alpha a} \delta(\tau - \tau'), \tag{3.13}$$

$$\frac{\partial G'_q(\boldsymbol{k}; \tau, \tau')}{\partial \tau} + \bar{\lambda} k^2 G'_q(\boldsymbol{k}; \tau, \tau')$$
$$- \mathrm{i} \iint \delta(\boldsymbol{k} - \boldsymbol{p} - \boldsymbol{q})\, \mathrm{d}\boldsymbol{p}\, \mathrm{d}\boldsymbol{q}\; N_{\mathrm{c}}^{\alpha bc} q^a u'^{\,b}_{\mathrm{B}}(\boldsymbol{p}; \tau) G'_q(\boldsymbol{q}; \tau, \tau') = \delta(\tau - \tau'), \tag{3.14}$$

$$\frac{\partial G'^{\,\alpha a}_b(\boldsymbol{k}; \tau, \tau')}{\partial \tau} + \bar{\eta} k^2 G'^{\,\alpha a}_b(\boldsymbol{k}; \tau)$$
$$- \mathrm{i} \iint \delta(\boldsymbol{k} - \boldsymbol{p} - \boldsymbol{q})\, \mathrm{d}\boldsymbol{p}\, \mathrm{d}\boldsymbol{q} N_{\mathrm{c}}^{\alpha bc} u'^{\,b}_{\mathrm{B}}(\boldsymbol{p}; \tau) G'^{\,ca}_b(\boldsymbol{q}; \tau) = \delta^{\alpha a} \delta(\tau - \tau'). \tag{3.15}$$

Note that these equations for the basic-field Green's functions are the same as the ones for homogeneous and isotropic MHD turbulence.

https://doi.org/10.1017/S0022377818001228 Published online by Cambridge University Press

In the following, we present the analytical results obtained in Paper 1 for the lowest-order fields $f'_0 = (\rho'_0, \boldsymbol{u}'_0, q'_0, \boldsymbol{b}'_0)$ and the first-order fields $f'_1 = (\rho'_1, \boldsymbol{u}'_1, q'_1, \boldsymbol{b}'_1)$.

With the Green's functions (3.12)–(3.15), the zeroth-order field $f'_0 = (\rho'_0, \boldsymbol{u}'_0, q'_0, \boldsymbol{b}'_0)$ can be solved in an iterative manner. The first iteration gives

$$\rho'_0(\boldsymbol{k};\tau) = \rho'_{\mathrm{B}}(\boldsymbol{k};\tau) + \mathrm{i}k^a\overline{\rho}\int_{-\infty}^{\tau}\mathrm{d}\tau_1 G'_\rho(\boldsymbol{k};\tau,\tau_1)u'_{\mathrm{B}}{}^a(\boldsymbol{k};\tau_1), \tag{3.16}$$

$$\begin{aligned} u'_0{}^\alpha(\boldsymbol{k};\tau) &= u'_{\mathrm{B}}{}^\alpha(\boldsymbol{k};\tau) + \mathrm{i}(\gamma_{\mathrm{s}}-1)k^a\int_{-\infty}^{\tau}\mathrm{d}\tau_1 G'_u{}^{\alpha a}(\boldsymbol{k};\tau,\tau_1)q'_{\mathrm{B}}(\boldsymbol{k};\tau_1) \\ &+ \mathrm{i}(\gamma_{\mathrm{s}}-1)\frac{Q}{\overline{\rho}}k^a\int_{-\infty}^{\tau}\mathrm{d}\tau_1 G'_u{}^{\alpha a}(\boldsymbol{k};\tau,\tau_1)\rho'_{\mathrm{B}}(\boldsymbol{k};\tau_1) \\ &+ \frac{\mathrm{i}}{\mu_0\overline{\rho}}\int_{-\infty}^{\tau}\mathrm{d}\tau_1 G'_u{}^{\alpha a}(\boldsymbol{k};\tau,\tau_1)\iint\delta(\boldsymbol{k}-\boldsymbol{p}-\boldsymbol{q})\,\mathrm{d}\boldsymbol{p}\,\mathrm{d}\boldsymbol{q}M_{\mathrm{c}}^{abc}b'_{\mathrm{B}}{}^b(\boldsymbol{p};\tau_1)b'_{\mathrm{B}}{}^c(\boldsymbol{q};\tau_1) \\ &- \frac{\mathrm{i}}{\mu_0\overline{\rho}}B^bk^b\int_{-\infty}^{\tau}\mathrm{d}\tau_1 G'_u{}^{\alpha a}(\boldsymbol{k};\tau,\tau_1)b'_{\mathrm{B}}{}^a(\boldsymbol{k};\tau_1), \end{aligned} \tag{3.17}$$

$$q'_0(\boldsymbol{k};\tau) = q_{\mathrm{B}}(\boldsymbol{k};\tau) + \mathrm{i}(\gamma_{\mathrm{s}}-1)Qk^a\int_{-\infty}^{\tau}\mathrm{d}\tau_1 G'_q(\boldsymbol{k};\tau,\tau_1)u'_{\mathrm{B}}{}^a(\boldsymbol{k};\tau_1), \tag{3.18}$$

$$\begin{aligned} b'_0{}^\alpha(\boldsymbol{k};\tau) &= b'_{\mathrm{B}}{}^\alpha(\boldsymbol{k};\tau) - \mathrm{i}B^bk^b\int_{-\infty}^{\tau}\mathrm{d}\tau_1 G'_b{}^{\alpha a}(\boldsymbol{k};\tau,\tau_1)u'_{\mathrm{B}}{}^a(\boldsymbol{k};\tau_1) \\ &+ \mathrm{i}B^ak^b\int_{-\infty}^{\tau}\mathrm{d}\tau_1 G'_b{}^{\alpha a}(\boldsymbol{k};\tau,\tau_1)u'_{\mathrm{B}}{}^b(\boldsymbol{k};\tau_1). \end{aligned} \tag{3.19}$$

Also, we formally solve the equations of $f'_1 = (\rho'_1, \boldsymbol{u}'_1, q'_1, \boldsymbol{b}'_1)$ to obtain

$$\begin{aligned} \rho'_1(\boldsymbol{k};\tau) &= \mathrm{i}k^a\overline{\rho}\int_{-\infty}^{\tau}\mathrm{d}\tau_1 G'_\rho(\boldsymbol{k};\tau,\tau_1)u'_{\mathrm{B}}{}^a(\boldsymbol{k};\tau_1) - \frac{\partial\overline{\rho}}{\partial X^a}\int_{-\infty}^{\tau}\mathrm{d}\tau_1 G'_\rho(\boldsymbol{k};\tau,\tau_1)u'_{\mathrm{B}}{}^a(\boldsymbol{k};\tau_1) \\ &- \frac{\partial U^b}{\partial X^b}\int_{-\infty}^{\tau}\mathrm{d}\tau_1 G'_\rho(\boldsymbol{k};\tau,\tau_1)\rho'_{\mathrm{B}}(\boldsymbol{k};\tau_1) - \int_{-\infty}^{\tau}\mathrm{d}\tau_1 G'_\rho(\boldsymbol{k};\tau,\tau_1)\frac{\mathrm{D}\rho'_{\mathrm{B}}(\boldsymbol{k};\tau_1)}{\mathrm{D}T} \\ &- \overline{\rho}\int_{-\infty}^{\tau}\mathrm{d}\tau_1 G'_\rho(\boldsymbol{k};\tau,\tau_1)\frac{\partial u'_{\mathrm{B}}{}^a(\boldsymbol{k};\tau_1)}{\partial X^a}, \end{aligned} \tag{3.20}$$

$$\begin{aligned} u'_1{}^\alpha(\boldsymbol{k};\tau) &= \mathrm{i}(\gamma_{\mathrm{s}}-1)k^a\int_{-\infty}^{\tau}\mathrm{d}\tau_1 G'_u{}^{\alpha a}(\boldsymbol{k};\tau,\tau_1)q'_1(\boldsymbol{k};\tau_1) \\ &+ \mathrm{i}(\gamma_{\mathrm{s}}-1)\frac{Q}{\overline{\rho}}k^a\int_{-\infty}^{\tau}\mathrm{d}\tau_1 G'_u{}^{\alpha a}(\boldsymbol{k};\tau,\tau_1)\rho'_1(\boldsymbol{k};\tau_1) \\ &+ \frac{2\mathrm{i}}{\mu_0\overline{\rho}}\int_{-\infty}^{\tau}\mathrm{d}\tau_1 G'_u{}^{\alpha a}(\boldsymbol{k};\tau,\tau_1)\iint\delta(\boldsymbol{k}-\boldsymbol{p}-\boldsymbol{q})\,\mathrm{d}\boldsymbol{p}\,\mathrm{d}\boldsymbol{q}M_{\mathrm{c}}^{abc}b'_0{}^b(\boldsymbol{p};\tau_1)b'_1{}^c(\boldsymbol{q};\tau_1) \\ &- \frac{\mathrm{i}}{\mu_0\overline{\rho}}B^bk^b\int_{-\infty}^{\tau}\mathrm{d}\tau_1 G'_u{}^{\alpha a}(\boldsymbol{k};\tau,\tau_1)b'_1{}^a(\boldsymbol{k};\tau_1) \\ &- \frac{\partial U^a}{\partial X^b}\int_{-\infty}^{\tau}\mathrm{d}\tau_1 G'_u{}^{\alpha a}(\boldsymbol{k};\tau,\tau_1)u'_0{}^b(\boldsymbol{k};\tau_1) \\ &- (\gamma_{\mathrm{s}}-1)\frac{1}{\overline{\rho}}\frac{\partial Q}{\partial X^a}\int_{-\infty}^{\tau}\mathrm{d}\tau_1 G'_u{}^{\alpha a}(\boldsymbol{k};\tau,\tau_1)\rho'_0(\boldsymbol{k};\tau_1) \end{aligned}$$

https://doi.org/10.1017/S0022377818001228 Published online by Cambridge University Press

$$
\begin{aligned}
&- (\gamma_{\mathrm{s}} - 1)\frac{1}{\overline{\rho}}\frac{\partial \overline{\rho}}{\partial X^a}\int_{-\infty}^{\tau} \mathrm{d}\tau_1 G'_u{}^{\alpha a}(\boldsymbol{k};\tau,\tau_1) q'_0(\boldsymbol{k};\tau_1)\\
&- \frac{1}{\mu_0\overline{\rho}}\frac{\partial B^a}{\partial X^b}\int_{-\infty}^{\tau} \mathrm{d}\tau_1 G'_u{}^{\alpha a}(\boldsymbol{k};\tau,\tau_1) b'_0{}^{b}(\boldsymbol{k};\tau_1)\\
&- \frac{1}{\overline{\rho}}\left(\frac{\partial U^a}{\partial T} + U^b\frac{\partial U^a}{\partial X^b}\right)\int_{-\infty}^{\tau} \mathrm{d}\tau_1 G'_u{}^{\alpha a}(\boldsymbol{k};\tau,\tau_1)\rho'_0(\boldsymbol{k};\tau_1), \qquad (3.21)
\end{aligned}
$$

$$
\begin{aligned}
q'_1(\boldsymbol{k};\tau) \;=\; & \mathrm{i}(\gamma_{\mathrm{s}} - 1)Qk^a\int_{-\infty}^{\tau} \mathrm{d}\tau_1 G'_q(\boldsymbol{k};\tau,\tau_1) u'_1{}^{a}(\boldsymbol{k};\tau_1)\\
&- \frac{\partial Q}{\partial X^a}\int_{-\infty}^{\tau} \mathrm{d}\tau_1 G'_q(\boldsymbol{k};\tau,\tau_1) u'_0{}^{a}(\boldsymbol{k};\tau_1)\\
&- (\gamma_{\mathrm{s}} - 1)\frac{\partial U^a}{\partial X^a}\int_{-\infty}^{\tau} \mathrm{d}\tau_1 G'_q(\boldsymbol{k};\tau,\tau_1) q'_0(\boldsymbol{k};\tau_1)\\
&- (\gamma_{\mathrm{s}} - 1)\frac{Q}{\overline{\rho}}\frac{\partial U^a}{\partial X^a}\int_{-\infty}^{\tau} \mathrm{d}\tau_1 G'_q(\boldsymbol{k};\tau,\tau_1) \rho'_0(\boldsymbol{k};\tau_1)\\
&- \int_{-\infty}^{\tau} \mathrm{d}\tau_1 G'_q(\boldsymbol{k};\tau,\tau_1)\frac{\mathrm{D}q'_0(\boldsymbol{k};\tau)}{\mathrm{D}T}\\
&- (\gamma_{\mathrm{s}} - 1)Q\int_{-\infty}^{\tau} \mathrm{d}\tau_1 G'_q(\boldsymbol{k};\tau,\tau_1)\frac{u'_0{}^{a}(\boldsymbol{k};\tau_1)}{\partial X^a}, \qquad (3.22)
\end{aligned}
$$

$$
\begin{aligned}
b'_1{}^{\alpha}(\boldsymbol{k};\tau) = & -\mathrm{i}B^b k^b\int_{-\infty}^{\tau} \mathrm{d}\tau_1 G'_b{}^{\alpha a}(\boldsymbol{k};\tau,\tau_1) u'_1{}^{a}(\boldsymbol{k};\tau_1)\\
&+ \mathrm{i}B^a k^b\int_{-\infty}^{\tau} \mathrm{d}\tau_1 G'_b{}^{\alpha a}(\boldsymbol{k};\tau,\tau_1) u_1{}'{}^{b}(\boldsymbol{k};\tau_1) - \frac{\partial B^a}{\partial X^b}\int_{-\infty}^{\tau} \mathrm{d}\tau_1 G'_b{}^{\alpha a}(\boldsymbol{k};\tau,\tau_1) u'_0{}^{b}(\boldsymbol{k};\tau_1)\\
&+ \frac{\partial U^a}{\partial X^b}\int_{-\infty}^{\tau} \mathrm{d}\tau_1 G'_b{}^{\alpha a}(\boldsymbol{k};\tau,\tau_1) b'_0{}^{b}(\boldsymbol{k};\tau_1) - \frac{\partial U^b}{\partial X^b}\int_{-\infty}^{\tau} \mathrm{d}\tau_1 G'_b{}^{\alpha a}(\boldsymbol{k};\tau,\tau_1) b'_0{}^{a}(\boldsymbol{k};\tau_1)\\
&- \int_{-\infty}^{\tau} \mathrm{d}\tau_1 G'_b{}^{\alpha a}(\boldsymbol{k};\tau,\tau_1)\frac{\mathrm{D}b'_0{}^{a}(\boldsymbol{k};\tau_1)}{\mathrm{D}T}\\
&+ B^b\int_{-\infty}^{\tau} \mathrm{d}\tau_1 G'_b{}^{\alpha a}(\boldsymbol{k};\tau,\tau_1)\frac{\partial u'_0{}^{a}(\boldsymbol{k};\tau_1)}{\partial X^b} - B^a\int_{-\infty}^{\tau} \mathrm{d}\tau_1 G'_b{}^{\alpha a}(\boldsymbol{k};\tau,\tau_1)\frac{\partial u'_0{}^{b}(\boldsymbol{k};\tau_1)}{\partial X^b}. \qquad (3.23)
\end{aligned}
$$

(v) Statistical assumption on the lowest-order fields

The lowest-order or basic fields $f'_{\mathrm{B}} = (\rho'_{\mathrm{B}}, \boldsymbol{u}'_{\mathrm{B}}, q'_{\mathrm{B}}, \boldsymbol{b}'_{\mathrm{B}})$ are homogeneous. We assume the homogeneous and isotropic properties for the basic-field statistics as

$$
\frac{\langle \rho'_{\mathrm{B}}(\boldsymbol{k};\tau)\rho'_{\mathrm{B}}(\boldsymbol{k}';\tau')\rangle}{\delta(\boldsymbol{k}+\boldsymbol{k}')} = \langle Q'_\rho(\boldsymbol{k};\tau,\tau')\rangle = Q_\rho(k;\tau,\tau'), \qquad (3.24)
$$

$$
\frac{\langle q'_{\mathrm{B}}(\boldsymbol{k};\tau)q'_{\mathrm{B}}(\boldsymbol{k}';\tau')\rangle}{\delta(\boldsymbol{k}+\boldsymbol{k}')} = \langle Q'_q(\boldsymbol{k};\tau,\tau')\rangle = Q_q(k;\tau,\tau'), \qquad (3.25)
$$

$$
\begin{aligned}
&\frac{\langle \vartheta'_{\mathrm{B}}{}^{\alpha}(\boldsymbol{k};\tau)\vartheta'_{\mathrm{B}}{}^{\beta}(\boldsymbol{k}';\tau')\rangle}{\delta(\boldsymbol{k}+\boldsymbol{k}')}\\
&\quad = D^{\alpha\beta}(\boldsymbol{k})Q_{\vartheta\vartheta\mathrm{S}}(k;\tau,\tau') + \Pi^{\alpha\beta}(\boldsymbol{k})Q_{\vartheta\vartheta\mathrm{C}}(k;\tau,\tau') + \frac{\mathrm{i}}{2}\frac{k^c}{k^2}\epsilon^{\alpha\beta c}H_{\vartheta\vartheta}(k;\tau,\tau'), \qquad (3.26)
\end{aligned}
$$

https://doi.org/10.1017/S0022377818001228 Published online by Cambridge University Press

$$\frac{1}{2\delta(\boldsymbol{k}+\boldsymbol{k}')}[\langle {u'_{\rm B}}^{\alpha}(\boldsymbol{k};\tau){b'_{\rm B}}^{\beta}(\boldsymbol{k}';\tau')\rangle+\langle {b'_{\rm B}}^{\alpha}(\boldsymbol{k};\tau){u'_{\rm B}}^{\beta}(\boldsymbol{k}';\tau')\rangle]$$
$$=D^{\alpha\beta}(\boldsymbol{k})Q_{w\rm S}(k;\tau,\tau')+\Pi^{\alpha\beta}(\boldsymbol{k})Q_{w\rm C}(k;\tau,\tau'), \tag{3.27}$$

where ϑ' represents either one of the velocity and magnetic-field fluctuations, $\boldsymbol{u}'$ and $\boldsymbol{b}'$, and $D^{\alpha\beta}$ and $\Pi^{\alpha\beta}$ are the solenoidal projection operator and the compressible counterpart defined by

$$D^{\alpha\beta}(\boldsymbol{k})=\delta^{\alpha\beta}-\frac{k^{\alpha}k^{\beta}}{k^2},\quad \Pi^{\alpha\beta}(\boldsymbol{k})=\frac{k^{\alpha}k^{\beta}}{k^2}. \tag{3.28a,b}$$

In (3.24)–(3.27), Q_{ρ}, Q_{q}, $Q_{\vartheta\vartheta\rm S}(\equiv Q_{\vartheta\rm S})$, $Q_{\vartheta\vartheta\rm C}(\equiv Q_{\vartheta\rm C})$, $Q_{w\rm S}$ and $Q_{w\rm C}$ are the spectral functions of the density variance, internal-energy variance, solenoidal and compressible parts of kinetic energy (for $\vartheta=u$) or magnetic energy (for $\vartheta=b$) and the counterparts of cross-helicity of the basic fields, respectively. Statistical properties (3.24)–(3.27) are natural extensions of the generic mathematical expressions for homogeneous isotropic turbulence (Batchelor 1953; Hinze 1975; Moffatt 1978; Lesieure 2008) to compressible MHD turbulence.

The second or $\Pi^{\alpha\beta}$-related terms: $Q_{u\rm C}$ in (3.26) with $\vartheta=u$ and $Q_{w\rm C}$ in (3.27), represent the turbulent kinetic energy and cross-helicity modes projected on to the wave vector $\boldsymbol{k}$. The physical origins of $Q_{u\rm C}$ and $Q_{w\rm C}$ are the non-solenoidal property of the compressional turbulent motion $\boldsymbol{u}'_{\rm C}$ ($\nabla\cdot\boldsymbol{u}'_{\rm C}\neq 0$). With the compressional motion $\boldsymbol{u}'_{\rm C}$, neither of the divergence of the velocity–velocity nor velocity–magnetic-field correlation tensors in the configuration space, $U^{\alpha\beta}(\boldsymbol{r},t)\equiv\langle u'^{\alpha}(\boldsymbol{x};t)u'^{\beta}(\boldsymbol{x}+\boldsymbol{r};t)\rangle$ nor $W^{\alpha\beta}(\boldsymbol{r},t)\equiv\langle u'^{\alpha}(\boldsymbol{x};t)b'^{\beta}(\boldsymbol{x}+\boldsymbol{r};t)\rangle$ vanishes even when the system is statistically isotropic:

$$\frac{\partial}{\partial r^{a}}U^{a\alpha}(\boldsymbol{r},t)=-\langle[\nabla\cdot\boldsymbol{u}'(\boldsymbol{x})]u'^{\alpha}(\boldsymbol{x}+\boldsymbol{r})\rangle=-\langle[\nabla\cdot\boldsymbol{u}'_{\rm C}(\boldsymbol{x})]u'^{\alpha}(\boldsymbol{x}+\boldsymbol{r})\rangle\neq 0, \tag{3.29}$$

$$\frac{\partial}{\partial r^{a}}W^{a\alpha}(\boldsymbol{r},t)=-\langle[\nabla\cdot\boldsymbol{u}'(\boldsymbol{x})]b'^{\alpha}(\boldsymbol{x}+\boldsymbol{r})\rangle=-\langle[\nabla\cdot\boldsymbol{u}'_{\rm C}(\boldsymbol{x})]b'^{\alpha}(\boldsymbol{x}+\boldsymbol{r})\rangle\neq 0. \tag{3.30}$$

These properties lead to the non-divergence-free spectral correlation tensor in wavenumber space, resulting in the compressional or $\Pi^{\alpha\beta}(=k^{\alpha}k^{\beta}/k^2)$-related parts of them, $Q_{u\rm C}$ in (3.26) and $Q_{w\rm C}$ in (3.27). These parts will be referred to as the compressional or dilatational energy and cross-helicity, respectively. A possible role of the dilatational cross-helicity will be argued later in § 5.

Under the assumptions of (3.24)–(3.27), they are related as

$$\langle {\rho'_{\rm B}}^{2}\rangle=\int Q_{\rho}(k;\tau,\tau)\,{\rm d}\boldsymbol{k}, \tag{3.31}$$

$$\langle {q'_{\rm B}}^{2}\rangle=\int Q_{q}(k;\tau,\tau)\,{\rm d}\boldsymbol{k}, \tag{3.32}$$

$$\langle {\boldsymbol{u}'_{\rm B}}^{2}\rangle/2=\int Q_{u}(k;\tau,\tau)\,{\rm d}\boldsymbol{k}=\int Q_{u\rm S}(k;\tau,\tau)\,{\rm d}\boldsymbol{k}+\int Q_{u\rm C}(k;\tau,\tau)\,{\rm d}\boldsymbol{k}, \tag{3.33}$$

$$\langle {\boldsymbol{b}'_{\rm B}}^{2}\rangle/2=\int Q_{b}(k;\tau,\tau)\,{\rm d}\boldsymbol{k}, \tag{3.34}$$

$$\langle \boldsymbol{u}'_{\rm B}\cdot\boldsymbol{b}'_{\rm B}\rangle=\int Q_{w}(k;\tau,\tau)\,{\rm d}\boldsymbol{k}.=\int Q_{w\rm S}(k;\tau,\tau)\,{\rm d}\boldsymbol{k}+\int Q_{w\rm C}(k;\tau,\tau)\,{\rm d}\boldsymbol{k}. \tag{3.35}$$

https://doi.org/10.1017/S0022377818001228 Published online by Cambridge University Press

(vi) Calculation of the correlations with renormalisation

The correlations in the configuration space are calculated from their counterparts in the wavenumber space as

$$\begin{aligned}\langle f'(\boldsymbol{x};t)g'(\boldsymbol{x};t)\rangle &= \int \mathrm{d}\boldsymbol{k}\langle f'(\boldsymbol{k};\tau)g'(\boldsymbol{k};\tau)\rangle/\delta(\boldsymbol{0}) \\ &= \int \mathrm{d}\boldsymbol{k}\left(\langle f'_0 g'_0\rangle + \langle f'_0 g'_1\rangle + \langle f'_1 g'_0\rangle + \cdots\right)/\delta(\boldsymbol{0}). \end{aligned} \tag{3.36}$$

From the formal solutions of the lowest- and first-order fields, equations (3.16)–(3.23), we can calculate the turbulent correlations.

Following the direct-interaction approximation (DIA), the basic-field propagators (bare propagators) are replaced with their exact counterparts in the calculations of the equations of the correlation and response functions (line renormalisation) (Kraichnan 1959).

In this formulation, the nonlinear coupling terms of the fluctuations are not truncated. This is marked contrast with the so-called quasi-linear or first-order smoothing approximations, where the nonlinear coupling terms with respect to the fluctuation fields are truncated. In the DIA formulation, the nonlinear coupling terms in the expansion series are evaluated by selecting the most important types of terms (direct interaction) in it and summing them to infinity (partial summation). This partial summation or renormalisation procedure is very useful in dealing with the strong nonlinearity in the turbulent field equations.

On the other hand, we introduced the concept of the basic fields, resulting in an uncoupled set of Green's functions by adding an infinitesimal disturbance to the nonlinear equations. The resulting equations of the Green's functions, (3.12)–(3.15), are in this sense linearised ones. Note that, by definition of Green's function, such linearisation is required for the superposition properties. Then the lowest-order fields coupled with each other are solved in an iterative manner.

4. Turbulent mass and internal-energy fluxes

4.1. *Turbulent mass flux*

The turbulent mass flux is calculated as

$$\begin{aligned}\langle \rho' \boldsymbol{u}'\rangle &= \langle \rho'_0 \boldsymbol{u}'_0\rangle + \langle \rho'_0 \boldsymbol{u}'_1\rangle + \langle \rho'_1 \boldsymbol{u}'_0\rangle + \cdots \\ &= \langle \rho'_{\mathrm{B}} \boldsymbol{u}'_{\mathrm{B}}\rangle + \langle \rho'_{\mathrm{B}} \boldsymbol{u}'_{01}\rangle + \langle \rho'_{\mathrm{B}} \boldsymbol{u}'_{10}\rangle + \cdots \\ &\quad + \langle \rho'_{01} \boldsymbol{u}'_{\mathrm{B}}\rangle + \langle \rho'_{01} \boldsymbol{u}'_{01}\rangle + \cdots + \langle \rho'_{10} \boldsymbol{u}'_{\mathrm{B}}\rangle + \cdots . \end{aligned} \tag{4.1}$$

From (3.16)–(3.23), each term in (4.1) is expressed as

$$\int \mathrm{d}\boldsymbol{k}\langle \rho'_{\mathrm{B}}(\boldsymbol{k};\tau) u'_{\mathrm{B}}{}^{\alpha}(-\boldsymbol{k};\tau)\rangle/\delta(\boldsymbol{0}) = 0, \tag{4.2}$$

$$\int \mathrm{d}\boldsymbol{k}\langle \rho'_{\mathrm{B}}(\boldsymbol{k};\tau) u'_{01}{}^{\alpha}(-\boldsymbol{k};\tau)\rangle/\delta(\boldsymbol{0}) = 0, \tag{4.3}$$

$$\begin{aligned}&\int \mathrm{d}\boldsymbol{k}\langle \rho'_{\mathrm{B}}(\boldsymbol{k};\tau) u'_{10}{}^{\alpha}(-\boldsymbol{k};\tau)\rangle/\delta(\boldsymbol{0}) \\ &= -\frac{1}{3}(\gamma_{\mathrm{s}}-1)\frac{1}{\bar{\rho}}\frac{\partial Q}{\partial X^{\alpha}}\int \mathrm{d}\boldsymbol{k}\int_{-\infty}^{\tau}\mathrm{d}\tau_1[2G_{u\mathrm{S}}(k;\tau,\tau_1)+G_{u\mathrm{C}}(k;\tau,\tau_1)]Q_{\rho}(k;\tau,\tau_1)\end{aligned}$$

https://doi.org/10.1017/S0022377818001228 Published online by Cambridge University Press

$$-\frac{1}{3}\frac{1}{\overline{\rho}}\frac{\mathrm{D}U^{\alpha}}{\mathrm{D}T}\int \mathrm{d}\boldsymbol{k}\int_{-\infty}^{\tau}\mathrm{d}\tau_1[2G_{u\mathrm{S}}(k;\tau,\tau_1)+G_{u\mathrm{C}}(k;\tau,\tau_1)]Q_{\rho}(k;\tau,\tau_1), \quad (4.4)$$

$$\int \mathrm{d}\boldsymbol{k}\langle\rho_{01}'(\boldsymbol{k};\tau)u_{\mathrm{B}}'^{\alpha}(-\boldsymbol{k};\tau)\rangle/\delta(\boldsymbol{0})=0, \quad (4.5)$$

$$\int \mathrm{d}\boldsymbol{k}\langle\rho_{1}'(\boldsymbol{k};\tau)u_{\mathrm{B}}'^{\alpha}(-\boldsymbol{k};\tau)\rangle/\delta(\boldsymbol{0})$$
$$=-\frac{1}{3}\frac{\partial\overline{\rho}}{\partial X^{\alpha}}\int \mathrm{d}\boldsymbol{k}\int_{-\infty}^{\tau}\mathrm{d}\tau_1 G_{\rho}(\boldsymbol{k};\tau,\tau_1)[2Q_{u\mathrm{S}}(k;\tau,\tau_1)+Q_{u\mathrm{C}}(k;\tau,\tau_1)], \quad (4.6)$$

$$\int \mathrm{d}\boldsymbol{k}\langle\rho_{01}'(\boldsymbol{k};\tau)u_{01}'^{\alpha}(-\boldsymbol{k};\tau)\rangle/\delta(\boldsymbol{0})$$
$$=-\frac{1}{3\mu_0}B^{\alpha}\int \mathrm{d}\boldsymbol{k}k^2\int_{-\infty}^{\tau}\mathrm{d}\tau_1\int_{-\infty}^{\tau}\mathrm{d}\tau_2 G_{\rho}(k;\tau,\tau_1)G_{u\mathrm{C}}(k;\tau,\tau_2)Q_{w\mathrm{C}}(k,\tau_1,\tau_2). \quad (4.7)$$

Here, we have used identity relations based on the properties of the solenoidal and compressional projection operators, $D^{\alpha\beta}$ and $\Pi^{\alpha\beta}$ (3.28), such as

$$k^a D^{\alpha a}=0, \quad (4.8)$$

$$\int \mathrm{d}\boldsymbol{k}k^a\Pi^{\alpha a}=\int \mathrm{d}\boldsymbol{k}k^a\frac{k^{\alpha}k^a}{k^2}=\int \mathrm{d}\boldsymbol{k}k^{\alpha}=0, \quad (4.9)$$

$$\int \mathrm{d}\boldsymbol{k}D^{\alpha a}=\frac{2}{3}\delta^{\alpha a}\int \mathrm{d}\boldsymbol{k}, \quad (4.10)$$

$$\int \mathrm{d}\boldsymbol{k}\Pi^{\alpha a}=\frac{1}{3}\delta^{\alpha a}\int \mathrm{d}\boldsymbol{k}, \quad (4.11)$$

$$D^{\alpha b}\Pi^{ab}=0, \quad (4.12)$$

$$\int \mathrm{d}\boldsymbol{k}k^a k^e\Pi^{\alpha b}\Pi^{ab}=\frac{1}{3}\delta^{e\alpha}\int \mathrm{d}\boldsymbol{k}. \quad (4.13)$$

These relations are mathematically rigorous and make the theoretical calculations accurate and simple by eliminating several coupling terms that give identically null contributions.

For the sake of brevity of description, we adopt the abbreviated forms of spectral and time integrals as

$$I_0\{A,B\}=\int \mathrm{d}\boldsymbol{k}\int_{-\infty}^{\tau}\mathrm{d}\tau_1 A(k;\tau,\tau_1)B(k;\tau,\tau_1), \quad (4.14)$$

$$I_{2n}\{A^{(1)},B^{(2)},C^{(2)}\}=\int \mathrm{d}\boldsymbol{k}k^{2n}\int_{-\infty}^{\tau}\mathrm{d}\tau_1\int_{-\infty}^{\tau}\mathrm{d}\tau_2 A(k;\tau,\tau_1)B(k;\tau,\tau_2)C(k;\tau_1,\tau_2). \quad (4.15)$$

It follows from (4.2)–(4.7) that the turbulent mass flux $\langle\rho'\boldsymbol{u}'\rangle$ is expressed as

$$\langle\rho'\boldsymbol{u}'\rangle=-\kappa_{\overline{\rho}}\nabla\overline{\rho}-\kappa_Q\nabla Q-\kappa_D\frac{\mathrm{D}\boldsymbol{U}}{\mathrm{D}T}-\kappa_B\boldsymbol{B}, \quad (4.16)$$

with the transport coefficients:

$$\kappa_{\overline{\rho}}=\tfrac{1}{3}I_0\{G_{\rho},2Q_{u\mathrm{S}}+Q_{u\mathrm{C}}\}, \quad (4.17)$$

https://doi.org/10.1017/S0022377818001228 Published online by Cambridge University Press

$$\kappa_Q = \frac{1}{3}(\gamma_s - 1)\frac{1}{\overline{\rho}} I_0\{2G_{u\mathrm{S}} + G_{u\mathrm{C}}, Q_\rho\}, \tag{4.18}$$

$$\kappa_D = \frac{1}{3}\frac{1}{\overline{\rho}} I_0\{2G_{u\mathrm{S}} + G_{u\mathrm{C}}, Q_\rho\}, \tag{4.19}$$

$$\kappa_B = \frac{1}{3\mu_0} I_1\{G_\rho^{(1)}, G_{u\mathrm{C}}^{(2)}, Q_{w\mathrm{C}}^{(2)}\}. \tag{4.20}$$

The first or $\kappa_{\overline{\rho}}$-related term in (4.16) corresponds to the so-called gradient-diffusion approximation of the turbulent mass flux. In the presence of the mean-density variation $\boldsymbol{\nabla}\overline{\rho}$, the mass flux due to turbulence occurs in the opposite direction to the mean-density gradient, and works so that it reduces the mean-density variation. The transport coefficient $\kappa_{\overline{\rho}}$ (4.17) is determined by the intensity of the turbulent motion represented by the spectra $Q_{u\mathrm{S}}$ and $Q_{u\mathrm{C}}$. The turbulent motions, both the solenoidal and compressional ones, contribute to this gradient diffusion of the mass.

The second or κ_Q-related term corresponds to the effective mass flux due to the mean internal energy, or equivalently the mean temperature variation, $\boldsymbol{\nabla}Q$, and may be called the cross-diffusion due to the internal-energy inhomogeneity. The transport coefficient κ_Q (4.18) is determined by the density-variance spectrum Q_ρ, and κ_Q as well as $\kappa_{\overline{\rho}}$ is always positive. This effect arises from strong compressibility. Depending on the relative configurations of the mean-density and internal-energy gradients, the cross-diffusion gives a deviation of the turbulent mass flux from the gradient diffusion due to the mean-density variation $\boldsymbol{\nabla}\overline{\rho}$. If the mean internal-energy or temperature gradient is in the opposite direction to the mean-density gradient, the mass flux might be effectively suppressed.

The third or κ_D-related term is the non-equilibrium mean velocity effect on the turbulent mass flux. A finite material derivative of the mean velocity $\mathrm{D}\boldsymbol{U}/\mathrm{D}t$ represents a non-equilibrium variation of the mean velocity. For instance, in the case of an impinging flow, $\mathrm{D}\boldsymbol{U}/\mathrm{D}t$ is negative in the direction of the flow impinging on the wall. Since the transport coefficient κ_D (4.19), which is determined by the density variance spectrum Q_ρ, is always positive, a negative $\mathrm{D}\boldsymbol{U}/\mathrm{D}t$ in impinging flow suggests an enhancement of the effective mass transport due to the density fluctuation.

The fourth or κ_B-related term represents the effective mass transport in the direction of the mean magnetic field $\boldsymbol{B}$. The transport coefficient κ_B (4.20) is determined by the compressional cross-helicity (i.e. the cross-helicity projected by the compressive projection Π) spectrum. This compressional cross-helicity corresponds to the part of the cross-helicity which is coupled with the dilatation/contraction fluctuation motions. Unlike $\kappa_{\overline{\rho}}$, κ_Q and κ_D, κ_B can be negative depending on the sign of the compressional cross-helicity. This term suggests that the mass is effectively transported by turbulence along the mean magnetic field $\boldsymbol{B}$. This effect also gives a possibility of the turbulent mass flux independent of the gradient of the mean density $\boldsymbol{\nabla}\overline{\rho}$. This effect will be further discussed in § 5.

4.2. *Turbulent internal-energy flux*

The turbulent heat flux is calculated as

$$\begin{aligned}\langle q'\boldsymbol{u}'\rangle &= \langle q'_0\boldsymbol{u}'_0\rangle + \langle q'_0\boldsymbol{u}'_1\rangle + \langle q'_1\boldsymbol{u}'_0\rangle + \cdots \\ &= \langle q'_{\mathrm{B}}\boldsymbol{u}'_{\mathrm{B}}\rangle + \langle q'_{\mathrm{B}}\boldsymbol{u}'_{01}\rangle + \langle q'_{\mathrm{B}}\boldsymbol{u}'_{10}\rangle + \cdots \\ &\quad + \langle q'_{01}\boldsymbol{u}'_{\mathrm{B}}\rangle + \langle q'_{01}\boldsymbol{u}'_{01}\rangle + \cdots + \langle q'_{10}\boldsymbol{u}'_{\mathrm{B}}\rangle + \cdots .\end{aligned} \tag{4.21}$$

https://doi.org/10.1017/S0022377818001228 Published online by Cambridge University Press

From (3.16)–(3.23), each term in (4.21) is expressed as

$$\int \mathrm{d}\boldsymbol{k}\langle q'_{\mathrm{B}}(\boldsymbol{k};\,\tau)u'_{\mathrm{B}}{}^{\alpha}(-\boldsymbol{k};\,\tau)\rangle/\delta(\boldsymbol{0})=0, \tag{4.22}$$

$$\int \mathrm{d}\boldsymbol{k}\langle q'_{\mathrm{B}}(\boldsymbol{k};\,\tau)u'_{01}{}^{\alpha}(-\boldsymbol{k};\,\tau)\rangle/\delta(\boldsymbol{0})=0, \tag{4.23}$$

$$\int \mathrm{d}\boldsymbol{k}\langle \rho'_{\mathrm{B}}(\boldsymbol{k};\,\tau)u'_{10}{}^{\alpha}(-\boldsymbol{k};\,\tau)\rangle/\delta(\boldsymbol{0})$$
$$=-\frac{1}{3}(\gamma_{\mathrm{s}}-1)\frac{1}{\overline{\rho}}\frac{\partial\overline{\rho}}{\partial X^{\alpha}}\int \mathrm{d}\boldsymbol{k}\int_{-\infty}^{\tau}\mathrm{d}\tau_1[2G_{u\mathrm{S}}(k;\,\tau,\,\tau_1)+G_{u\mathrm{C}}(k;\,\tau,\,\tau_1)]Q_q(k;\,\tau,\,\tau_1), \tag{4.24}$$

$$\int \mathrm{d}\boldsymbol{k}\langle q'_{01}(\boldsymbol{k};\,\tau)u'_{\mathrm{B}}{}^{\alpha}(-\boldsymbol{k};\,\tau)\rangle/\delta(\boldsymbol{0})=0, \tag{4.25}$$

$$\int \mathrm{d}\boldsymbol{k}\langle q'_{1}(\boldsymbol{k};\,\tau)u'_{\mathrm{B}}{}^{\alpha}(-\boldsymbol{k};\,\tau)\rangle/\delta(\boldsymbol{0})$$
$$=-\frac{\partial Q}{\partial X^{\alpha}}\frac{1}{3}\int \mathrm{d}\boldsymbol{k}\int_{-\infty}^{\tau}\mathrm{d}\tau_1 G_q(k;\,\tau,\,\tau_1)[2Q_{u\mathrm{S}}(k;\,\tau,\,\tau_1)+Q_{u\mathrm{C}}(k;\,\tau,\,\tau_1)], \tag{4.26}$$

$$\int \mathrm{d}\boldsymbol{k}\langle q'_{01}(\boldsymbol{k};\,\tau)u'_{01}{}^{\alpha}(-\boldsymbol{k};\,\tau)\rangle/\delta(\boldsymbol{0})=-\frac{1}{3}\frac{1}{\mu_0\overline{\rho}}(\gamma_s-1)Q\int \mathrm{d}\boldsymbol{k}k^2\int_{-\infty}^{\tau}\mathrm{d}\tau_1\int_{-\infty}^{\tau}\mathrm{d}\tau_2$$
$$\times G_q(k;\,\tau,\,\tau_1)G_{u\mathrm{C}}(k;\,\tau,\,\tau_2)Q_{w\mathrm{C}}(k;\,\tau_1,\,\tau_2)B^{\alpha}. \tag{4.27}$$

It follows from (4.22)–(4.27) that the turbulent internal-energy flux $\langle q'\boldsymbol{u}'\rangle$ is expressed as

$$\langle q'\boldsymbol{u}'\rangle=-\eta_Q\boldsymbol{\nabla}Q-\eta_{\overline{\rho}}\boldsymbol{\nabla}\overline{\rho}-\eta_B\boldsymbol{B}, \tag{4.28}$$

with the transport coefficients:

$$\eta_Q=\tfrac{1}{3}I_0\{G_q,\,2Q_{u\mathrm{S}}+Q_{u\mathrm{C}}\}, \tag{4.29}$$

$$\eta_{\overline{\rho}}=\frac{1}{3}(\gamma_{\mathrm{s}}-1)\frac{1}{\overline{\rho}}I_0\{2G_{u\mathrm{S}}+G_{u\mathrm{C}},\,Q_q\}, \tag{4.30}$$

$$\eta_B=\frac{1}{3\mu_0\overline{\rho}}(\gamma_{\mathrm{s}}-1)QI_1\{G_q^{(1)},\,G_{u\mathrm{C}}^{(2)},\,Q_{w\mathrm{C}}^{(2)}\}. \tag{4.31}$$

The first or η_Q-related term in (4.28) represents the gradient diffusion of the internal energy. In the presence of the mean internal-energy gradient $\boldsymbol{\nabla}Q$, the effective energy transport, mediated by the turbulent motions, is in the direction reducing the inhomogeneity of the internal energy. The transport coefficient η_Q (4.29) is determined by the solenoidal and compressional components of the spectral functions of the turbulent motions.

The second or $\eta_{\overline{\rho}}$-related term represents the turbulent internal-energy flux due to the mean-density gradient $\boldsymbol{\nabla}\overline{\rho}$. In addition to the gradient diffusion due to $\boldsymbol{\nabla}Q$, a gradient of the mean density, $\boldsymbol{\nabla}\overline{\rho}$, may contribute to the internal-energy transport through the fluctuation of the internal energy. This is a *cross-diffusion* term; depending on the relative configurations of $\boldsymbol{\nabla}\overline{\rho}$ and $\boldsymbol{\nabla}Q$, the turbulent internal-energy flux can deviate from the simple gradient diffusion proportional to $\boldsymbol{\nabla}Q$. The transport

https://doi.org/10.1017/S0022377818001228 Published online by Cambridge University Press

coefficient $\eta_{\overline{\rho}}$ (4.30) is determined by the spectral function of the internal-energy variance Q_q, which is directly related to the density-variance spectrum Q_ρ or the density variance itself $\langle \rho'^2 \rangle$ as we see for the modelling of this effect in § 4.3.

The third or η_B-related term gives a possibility of enhancing the turbulent internal-energy flux along the mean magnetic field $\boldsymbol{B}$. The transport coefficient η_B (4.31) is determined by the spectral function of the compressional part of the turbulent cross-helicity. Unlike the spectral functions of the turbulent energy Q_u and the turbulent internal-energy Q_q, $Q_{w\mathrm{C}}$ is not positive definite. Hence, the transport coefficient η_B can be positive or negative depending on the sign of the turbulent compressional cross-helicity. This term makes it possible for the internal energy to transport independently of the gradient of the mean internal energy ∇Q or the gradient of the mean density $\nabla \overline{\rho}$. The physical origin of this effect is related to the magnetohydrodynamic (MHD) wave effect. We discuss this point later in § 5.

4.3. *Modelling turbulent fluxes*

In order to properly evaluate the mean-field quantities, $\overline{\rho}$, $\boldsymbol{U}$, Q and $\boldsymbol{B}$, from their transport equations (2.14)–(2.15) and (2.17)–(2.18), we need the expressions for the turbulent correlations. For example, the turbulent mass flux $\langle \rho' \boldsymbol{u}' \rangle$ and the turbulent internal-energy flux $\langle q' \boldsymbol{u}' \rangle$ provide essential contributions to the evolution of the mean internal energy (2.17). The theoretical results for $\langle \rho' \boldsymbol{u}' \rangle$ (4.16) and $\langle q' \boldsymbol{u}' \rangle$(4.28) with the analytical expressions of the transport coefficients (4.17)–(4.20) and (4.29)–(4.31) are written in terms of the spectral and time integrals of the Green's functions and spectral functions of MHD turbulence. For practical applications these analytical expressions are too heavy, so we construct a turbulence model with one-point quantities on the basis of the analytical results.

The Green's functions represent how much the past states affect the present states. The characteristic times of turbulence may be defined with the aid of the Green's functions as

$$\tau_s = \int_{-\infty}^{\tau} \mathrm{d}\tau_1 \langle G'_s(\boldsymbol{k}; \tau, \tau_1) \rangle = \int_{-\infty}^{\tau} \mathrm{d}\tau_1 G_s(\boldsymbol{k}; \tau, \tau_1), \tag{4.32}$$

with $s = (\rho, u, q, b)$. Utilising these time scales, the transport coefficients $\kappa_{\overline{\rho}}$ (4.17), κ_Q (4.18), κ_D (4.19), κ_B (4.20), η_Q (4.29), $\eta_{\overline{\rho}}$ (4.30) and η_B (4.31) may be modelled as

$$\kappa_{\overline{\rho}} = C_{\kappa\rho} \tau_\rho \langle \boldsymbol{u}'^2 \rangle / 2, \tag{4.33}$$

$$\kappa_Q = C_{\kappa Q} (\gamma_\mathrm{s} - 1) \tau_u \overline{\rho} \frac{\langle \rho'^2 \rangle}{\overline{\rho}^2}, \tag{4.34}$$

$$\kappa_D = C_{\kappa D} \tau_u \overline{\rho} \frac{\langle \rho'^2 \rangle}{\overline{\rho}^2}, \tag{4.35}$$

$$\kappa_B = C_{\kappa B} \frac{1}{\mu_0 \overline{\rho}} \tau_\rho \tau_{uc} \overline{\rho} \langle \boldsymbol{u}' \cdot \boldsymbol{b}' \rangle_\mathrm{C}, \tag{4.36}$$

$$\eta_Q = C_{\eta Q} \tau_q \langle \boldsymbol{u}'^2 \rangle / 2, \tag{4.37}$$

$$\eta_{\overline{\rho}} = C_{\eta\rho} (\gamma_\mathrm{s} - 1) \tau_u \frac{\langle q'^2 \rangle}{\overline{\rho}} = C_{\eta\rho} (\gamma_\mathrm{s} - 1)^3 \frac{\tau_u \tau_q^2}{\tau_\rho^2} \frac{Q^2}{\overline{\rho}} \frac{\langle \rho'^2 \rangle}{\overline{\rho}^2}, \tag{4.38}$$

$$\eta_B = C_{\eta B} \frac{1}{\mu_0 \overline{\rho}} (\gamma_\mathrm{s} - 1) \tau_q \tau_{uc} Q \langle \boldsymbol{u}' \cdot \boldsymbol{b}' \rangle_\mathrm{C}. \tag{4.39}$$

https://doi.org/10.1017/S0022377818001228 Published online by Cambridge University Press

In the second equality of (4.38), use has been made of the approximate relations:

$$q' \simeq -(\gamma_s - 1)\tau_q Q \nabla \cdot \boldsymbol{u}' \tag{4.40}$$

and

$$\nabla \cdot \boldsymbol{u}' \simeq -\frac{1}{\tau_\rho}\frac{\rho'}{\overline{\rho}} \tag{4.41}$$

(see (2.19) and (2.21) with (3.16) and (3.18)).

The gradient-diffusion-related coefficients $\kappa_{\overline{\rho}}$ (4.33) and η_Q (4.37) are determined by the turbulent energy $\langle \boldsymbol{u}'^2 \rangle/2$, which includes both solenoidal and compressive fluctuation motions. These effects are present even in the solenoidal case. The cross-diffusion effects κ_Q (4.34) and $\eta_{\overline{\rho}}$ (4.38) and the non-equilibrium effect κ_D (4.35) ddepend on the density variance $\langle \rho'^2 \rangle$, which is expected to be relevant in strongly compressible turbulence. The turbulent mass and internal-energy fluxes along the mean magnetic field $\boldsymbol{B}$, κ_B (4.36) and η_B (4.39), are determined by the compressional part of the turbulent cross-helicity, $\langle \boldsymbol{u}' \cdot \boldsymbol{b}' \rangle_C$. These compressional turbulent cross-helicity effects (i.e. cross-helicity effects coupled with the compressible motions) are further discussed in the following section (§ 5).

4.4. *Correspondence to turbulent entropy flux*

In the astrophysical and geophysical contexts, the entropy s, in place of the internal energy q, is often adopted as one of the key statistical quantities. From the first law of thermodynamics:

$$\mathrm{d}q = -p d(1/\rho) + \theta \, \mathrm{d}s, \tag{4.42}$$

the evolution equation of s is written as

$$\theta \frac{\mathrm{D}s}{\mathrm{D}t} = \frac{\mathrm{D}q}{\mathrm{D}t} + p \frac{\mathrm{D}}{\mathrm{D}t}\frac{1}{\rho} = \frac{\mathrm{D}q}{\mathrm{D}t} - \frac{p}{\rho^2}\frac{\mathrm{D}\rho}{\mathrm{D}t} \tag{4.43}$$

in relation with the equations of the internal energy and density, q and ρ (Mihalas & Weibel-Mihalas 1984).

Applying ensemble or Reynolds decomposition of the variables θ, s, q, p and ρ into (4.43) and taking an average, we obtain the evolution equation of the mean entropy, S, which contains the convective flux $\langle s' \boldsymbol{u}' \rangle$ contribution. An elaborated analysis of the expression of the turbulent entropy flux $\langle s' \boldsymbol{u}' \rangle$ requires another paper, but from (4.43), the turbulent entropy flux may be approximated as

$$\langle s' \boldsymbol{u}' \rangle = \frac{1}{\Theta}\langle q' \boldsymbol{u}' \rangle - \frac{1}{\Theta}\frac{P}{\overline{\rho}^2}\langle \rho' \boldsymbol{u}' \rangle. \tag{4.44}$$

The expressions of the turbulent fluxes of the internal energy and mass, $\langle q' \boldsymbol{u}' \rangle$ (4.28) and $\langle \rho' \boldsymbol{u}' \rangle$ (4.16), suggest that the primary part of the expression of $\langle s' \boldsymbol{u}' \rangle$ may be written as

$$\langle s' \boldsymbol{u}' \rangle = -\eta_Q \frac{1}{\Theta}\nabla Q + \kappa_{\overline{\rho}}\frac{1}{\Theta}\frac{P}{\overline{\rho}^2}\nabla \overline{\rho}. \tag{4.45}$$

With the expressions for the transport coefficients η_Q (4.29) and $\kappa_{\overline{\rho}}$ (4.17), and their models (4.37) and (4.33), the turbulent entropy flux may be modelled as

$$\langle s' \boldsymbol{u}' \rangle = -\chi_S \nabla S, \tag{4.46}$$

https://doi.org/10.1017/S0022377818001228 Published online by Cambridge University Press

where χ_S is the transport coefficient proportional to the turbulent kinetic energy $\langle \boldsymbol{u}'^2 \rangle / 2$. This expression is similar to the one obtained by Rogachevskii & Kleeorin (2015) for low Mach number flows. Note that, among several transport coefficients, the gradient-diffusion coefficients, η_Q and $\kappa_{\overline{\rho}}$, arise even in the case of no or weak compressibility. Of course, the full expressions for $\langle \rho' \boldsymbol{u}' \rangle$ (4.28) and $\langle q' \boldsymbol{u}' \rangle$ (4.16) infer some additional terms for $\langle s' \boldsymbol{u}' \rangle$. A more elaborated analysis in the context of astrophysical and geophysical applications will be reported in the future.

With (4.43), we construct the mean entropy $\overline{\rho} S$ equation ($S = \langle s \rangle$) (Braginsky & Roberts 1995; Rogachevskii & Kleeorin 2015). In the mean entropy equation, we have the turbulent flux of entropy $\overline{\rho} \langle s' \boldsymbol{u}' \rangle$. In some of the literature, the effect of the entropy flux is expressed by $(1/\Theta) \boldsymbol{\nabla} \cdot \Theta \overline{\rho} \langle s' \boldsymbol{u}' \rangle$, which coincides with the formulation with the turbulent flux of internal energy. From the definition of the entropy (4.42) and the equation of state (2.8) with (2.9), the internal-energy fluctuation is written as

$$q' = \left[s' + C_V (\gamma_s - 1) \frac{\rho'}{\overline{\rho}} \right] \Theta. \tag{4.47}$$

The convective flux $\Theta \overline{\rho} \langle s' \boldsymbol{u}' \rangle$, which is often used in the current studies, corresponds to the second term on the right-hand side in (2.17) with the low Mach number approximation of (4.47) ($q' = \Theta s'$).

5. Dilatational cross-helicity effects and magnetohydrodynamic waves

5.1. *Dilatational cross-helicity effects*

The fourth term in (4.16) and the third term in (4.28) imply possibilities of the turbulent mass and internal-energy fluxes along the mean magnetic field, respectively. They deserve further consideration, since they may lead to deviations from the gradient-diffusion approximation for the turbulent fluxes, expressed by $\boldsymbol{\nabla} \overline{\rho}$ in $\langle \rho' \boldsymbol{u}' \rangle$ and $\boldsymbol{\nabla} Q$ in $\langle q' \boldsymbol{u}' \rangle$, in the compressible MHD turbulence.

As we saw in (4.20) and (4.31) and their models (4.36) and (4.39), the transport coefficients κ_B and η_B are expressed and modelled as

$$\begin{aligned} \kappa_B &= \frac{1}{3\mu_0} \int \mathrm{d}\boldsymbol{k} k^2 \int_{-\infty}^{\tau} \mathrm{d}\tau_1 \int_{-\infty}^{\tau} \mathrm{d}\tau_2 G_\rho(k; \tau, \tau_1) G_{uc}(k; \tau, \tau_2) Q_{w\mathrm{C}}(k; \tau_1, \tau_2) \\ &\equiv \frac{1}{3\mu_0} I_1\{G_\rho^{(1)}, G_{u\mathrm{C}}^{(2)}, Q_{w\mathrm{C}}^{(2)}\} \\ &= C_{\kappa B} \frac{1}{\mu_0 \overline{\rho}} \tau_\rho \tau_{uc} \overline{\rho} \langle \boldsymbol{u}' \cdot \boldsymbol{b}' \rangle_{\mathrm{C}} \end{aligned} \tag{5.1}$$

and

$$\begin{aligned} \eta_B &= \frac{1}{3\mu_0} \int \mathrm{d}\boldsymbol{k} k^2 \int_{-\infty}^{\tau} \mathrm{d}\tau_1 \int_{-\infty}^{\tau} \mathrm{d}\tau_2 G_q(k; \tau, \tau_1) G_{uc}(k; \tau, \tau_2) Q_{w\mathrm{C}}(k; \tau_1, \tau_2) \\ &\equiv \frac{1}{3\mu_0} I_1\{G_q^{(1)}, G_{u\mathrm{C}}^{(2)}, Q_{w\mathrm{C}}^{(2)}\} \\ &= C_{\eta B} \frac{1}{\mu_0 \overline{\rho}} (\gamma_s - 1) \tau_q \tau_{uc} Q \langle \boldsymbol{u}' \cdot \boldsymbol{b}' \rangle_{\mathrm{C}}, \end{aligned} \tag{5.2}$$

where τ_ρ, τ_q and τ_{uc} are the characteristic time scales of the density, internal energy and compressible velocity evolutions. The transport coefficients κ_B and η_B coupled

https://doi.org/10.1017/S0022377818001228 Published online by Cambridge University Press

with the mean magnetic field $\boldsymbol{B}$ are constituted of the compressional or dilatational part of the turbulent cross-helicity, $\langle \boldsymbol{u}' \cdot \boldsymbol{b}' \rangle_{\mathrm{C}}$. In order for these effects to work, both the compressibility and the cross-correlation between the velocity and magnetic-field fluctuations should present simultaneously.

For the compressional cross-helicity effects, fluid dynamics related to the dilatational motions $\nabla \cdot \boldsymbol{u}'_{\mathrm{C}}$ should play an essential role. To get a deeper understanding of these turbulent transports along the mean magnetic field, we first examine the turbulent mass flux $\langle \rho' \boldsymbol{u}' \rangle$ by considering a simple situation of the density and velocity fluctuations. From the fluctuation equations of the density ρ' (2.19) and the velocity $\boldsymbol{u}'$ (2.20), the time evolution of ρ' and $\boldsymbol{u}'$ are respectively approximated as

$$\frac{\mathrm{D}\rho'}{\mathrm{D}t} \simeq -\overline{\rho} \nabla \cdot \boldsymbol{u}', \tag{5.3}$$

$$\frac{\mathrm{D}\boldsymbol{u}'}{\mathrm{D}t} \simeq \frac{1}{\mu_0 \overline{\rho}} (\boldsymbol{B} \cdot \nabla) \boldsymbol{b}'. \tag{5.4}$$

These can be integrated with respect to time, and the variations of the density fluctuation and velocity fluctuation, $\delta\rho'$ and $\delta\boldsymbol{u}'$, are primarily expressed as

$$\delta\rho' \simeq -\tau_\rho \overline{\rho} \nabla \cdot \boldsymbol{u}', \tag{5.5}$$

$$\delta\boldsymbol{u}' \simeq \tau_u \frac{1}{\mu_0 \overline{\rho}} (\boldsymbol{B} \cdot \nabla) \boldsymbol{b}', \tag{5.6}$$

with some other constraints such as the solenoidal condition of the magnetic-field fluctuation $\nabla \cdot \boldsymbol{b}' = 0$. As we see from (2.19) and its expanded expression in the wavenumber space (3.16), the density fluctuation ρ' is directly related to the turbulent dilatation/contraction $\nabla \cdot \boldsymbol{u}'$. Also the magnetic fluctuation being inhomogeneous along the mean magnetic field, $(\boldsymbol{B} \cdot \nabla)\boldsymbol{b}'$, may lead to the variation of the velocity fluctuation $\delta\boldsymbol{u}'$ along the direction of the magnetic fluctuation variation. For evaluating the turbulent mass flux $\langle \rho' \boldsymbol{u}' \rangle$, we utilise these expressions.

We consider a compressible fluid plasma element located in a uniform mean magnetic field $\boldsymbol{B}$ (figure 1). Because of the compressibility, we have a finite turbulent dilatation/contraction ($\nabla \cdot \boldsymbol{u}' \neq 0$). Note that the magnitude of the density fluctuation depends on the strength of the compressibility. By considering the equation of the density variance $\langle \rho'^2 \rangle$, we expect a large density fluctuation at a location with a large mean-density variation (see arguments in § 6 of Paper 1). In the expansion or positive turbulent dilatation case ($\nabla \cdot \boldsymbol{u}' > 0$), the variation of the density fluctuation $\delta\rho$ is negative as

$$\delta\rho' = -\tau_\rho \overline{\rho} \nabla \cdot \boldsymbol{u}' < 0 \tag{5.7}$$

(figure 1*a*,*c*).

Note that, in general, both $\boldsymbol{u}'_{\mathrm{C}}$ (compressible component of $\boldsymbol{u}'$) and the solenoidal magnetic-field fluctuation $\boldsymbol{b}'$ have components in the direction of the mean magnetic field $\boldsymbol{B}$. First we assume that the turbulent cross-helicity associated with the turbulent dilatation is positive ($\langle \boldsymbol{u}' \cdot \boldsymbol{b}' \rangle_{\mathrm{C}} > 0$). This corresponds to a situation where the magnetic fluctuation $\boldsymbol{b}'$ longitudinal to the mean magnetic field $\boldsymbol{B}$ is statistically aligned with the counterpart of the velocity fluctuation $\boldsymbol{u}'$ (figure 1*a*). Because of this assumption of positive compressional cross-helicity, the direction of the longitudinal magnetic fluctuation $\boldsymbol{b}'_{\parallel}$ is statistically aligned with the longitudinal velocity fluctuation $\boldsymbol{u}'_{\parallel}$ (the suffix $\parallel$ denotes the component along the mean magnetic field $\boldsymbol{B}$). For a positive

https://doi.org/10.1017/S0022377818001228 Published online by Cambridge University Press

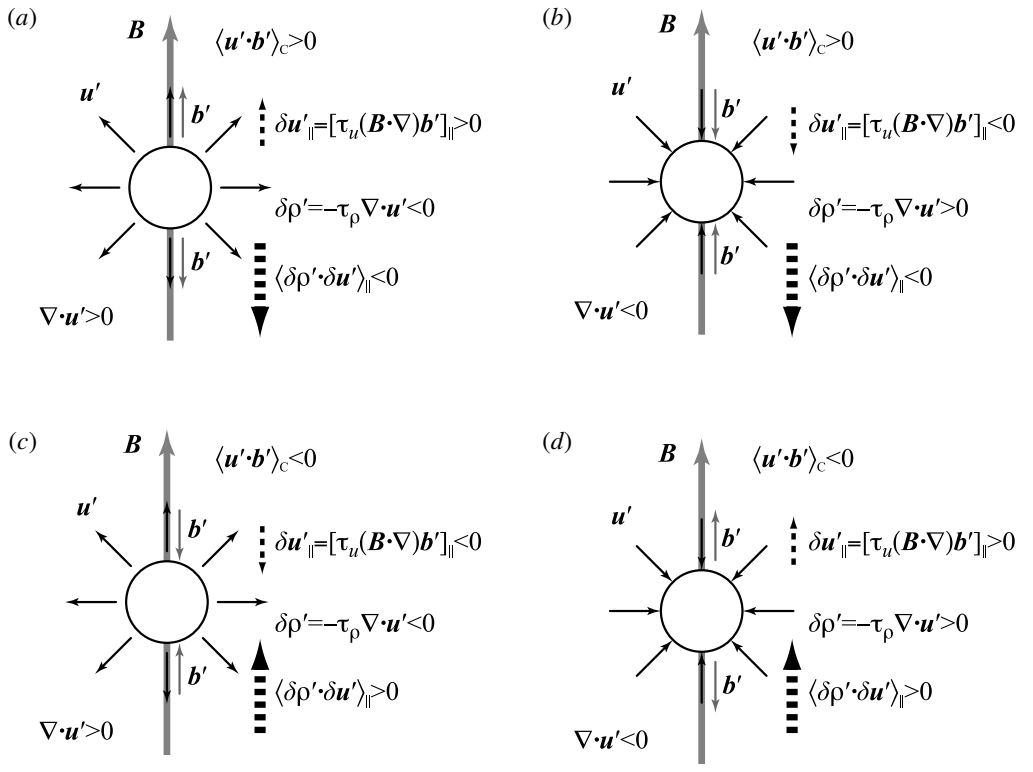

FIGURE 1. Compressional cross-helicity effect. (*a*) Dilatation and positive compressional cross-helicity (CCH) ($\nabla \cdot \boldsymbol{u}' > 0$ and $\langle \boldsymbol{u}' \cdot \boldsymbol{b}' \rangle_C > 0$); (*b*) contraction and positive CCH ($\nabla \cdot \boldsymbol{u}' < 0$ and $\langle \boldsymbol{u}' \cdot \boldsymbol{b}' \rangle_C > 0$); (*c*) dilatation and negative CCH ($\nabla \cdot \boldsymbol{u}' > 0$ and $\langle \boldsymbol{u}' \cdot \boldsymbol{b}' \rangle_C < 0$); (*d*) contraction and negative CCH ($\nabla \cdot \boldsymbol{u}' < 0$ and $\langle \boldsymbol{u}' \cdot \boldsymbol{b}' \rangle_C < 0$).

compressional cross-helicity ($\langle \boldsymbol{u}' \cdot \boldsymbol{b}' \rangle_C > 0$), an expansion for the plasma along $\boldsymbol{B}$ ($\nabla \cdot \boldsymbol{u}'_\parallel > 0$) is statistically equivalent to $\nabla \cdot \boldsymbol{b}'_\parallel > 0$. In this case, as shown by the thin dashed line in figure 1(*a*), the variation of the velocity fluctuation (5.6) is positive in the direction of $\boldsymbol{B}$ as

$$\delta u'_\parallel = \tau_u \frac{1}{\mu_0 \overline{\rho}} (\boldsymbol{B} \cdot \nabla) b'_\parallel > 0. \tag{5.8}$$

Note that because of the solenoidal property of the magnetic field, $\nabla \cdot \boldsymbol{b}' = 0$ should be always satisfied. It follows from (5.7) and (5.8) that the turbulent mass flux estimated by $\langle \delta\rho' \delta \boldsymbol{u}' \rangle$ due to the compressional turbulent cross-helicity is along the mean magnetic field but antiparallel to $\boldsymbol{B}$ (thick dashed line in figure 1*a*). In the contraction or negative dilatation case ($\nabla \cdot \boldsymbol{u}' < 0$), $\delta\rho'$ in (5.7) turns out to be positive while $\delta u'_\parallel$ in (5.8) becomes negative. As a result, $\langle \delta\rho' \delta \boldsymbol{u}' \rangle$ is exactly the same as in the expansion or positive dilatation case (figure 1*b*). Irrespective of the sign of the turbulent dilatation, the turbulent mass flux $\langle \rho' \boldsymbol{u}' \rangle$ due to the coupling of the mean magnetic field $\boldsymbol{B}$ and compressional cross-helicity $\langle \boldsymbol{u}' \cdot \boldsymbol{b}' \rangle_C$ is along but antiparallel to $\boldsymbol{B}$ as long as the $\langle \boldsymbol{u}' \cdot \boldsymbol{b}' \rangle_C > 0$ is positive (figure 1*a*,*b*).

On the other hand, for the negative compressional cross-helicity ($\langle \boldsymbol{u}' \cdot \boldsymbol{b}' \rangle_C < 0$), the turbulent mass flux due to the compressional cross-helicity effect is along and parallel to the mean magnetic field $\boldsymbol{B}$ (figure 1*c*,*d*).

https://doi.org/10.1017/S0022377818001228 Published online by Cambridge University Press

This is a simplified explanation for the fourth or κ_B-related term in (4.16) with the transport coefficient (4.20) or the model expression (4.36):

$$\langle \rho' \boldsymbol{u}' \rangle_B = -\kappa_B \boldsymbol{B}, \tag{5.9}$$

with κ_B being proportional to the compressional cross-helicity (5.1).

Entirely similar arguments can be made for the turbulent internal-energy flux $\langle q' \boldsymbol{u}' \rangle$. In this case, the equation of the turbulent internal energy (2.21) should be used in place of the equation of the turbulent density (2.19). Equation (5.3) is replaced by the time evolution of q' approximated by

$$\frac{\mathrm{D}q'}{\mathrm{D}t} \simeq -(\gamma_s - 1) Q \boldsymbol{\nabla} \cdot \boldsymbol{u}' \tag{5.10}$$

from (2.21). The variation of the turbulent internal-energy, $\delta q'$, can be estimated as

$$\delta q' \simeq -\tau_q (\gamma_s - 1) Q \boldsymbol{\nabla} \cdot \boldsymbol{u}' \tag{5.11}$$

from (3.18). Then, the turbulent internal-energy flux is given as

$$\langle q' \boldsymbol{u}' \rangle_B = -\eta_B \boldsymbol{B}, \tag{5.12}$$

with η_B being (5.2). As with the turbulent mass flux $\langle \rho' \boldsymbol{u}' \rangle_B$, the turbulent internal-energy flux $\langle q' \boldsymbol{u}' \rangle_B$ is along the mean magnetic field $\boldsymbol{B}$ in the opposite (or same) direction to $\boldsymbol{B}$ for the positive (or negative) dilatational cross-helicity. Irrespective of the sign of the turbulent dilatation, the direction of the internal-energy flux is determined by the sign of the dilatational turbulent cross-helicity. One interesting point is that in the isothermal process ($\gamma_s = 1$) this internal-energy transport due to the dilatational cross-helicity does not show up, since in this case the internal-energy variation due to the turbulent dilatation disappears as (5.11).

Here we should note that, in the above physical pictures, the sign of the dilatational turbulent cross-helicity is just assumed or prescribed. In reality, turbulent fields including the velocity and magnetic-field fluctuations evolve subjected to the nonlinear dynamics of the MHD turbulence with inhomogeneous mean fields. A self-consistent treatment of the spatio-temporal evolution of the turbulent cross-helicity can be done only by solving the transport equation of the turbulent cross-helicity under the mutual influence of the mean and turbulence fields (e.g. see Yokoi & Hoshino 2011; Yokoi 2013). This point will be argued later in § 6. However, in the linearised MHD equations, the perturbations including the velocity and magnetic-field ones obey definite and specific modes following the dispersion relations. Since those linear wave arguments provide us with some understanding on the dilatational turbulent cross-helicity effect, we present such arguments in the following subsection, § 5.2.

5.2. *Magnetohydrodynamic waves*

In the presence of the mean magnetic field $\boldsymbol{B}$, the time-dependent disturbances of the velocity and magnetic fields are propagated as magnetohydrodynamic (MHD) waves. If we restrict our attention to small-amplitude disturbances, we can consider small-scale perturbations as wave-like solutions of the linearised MHD equations.

As is shown in appendix A, the dispersion relation (A 12) has three roots. One is the transverse or shear Alfvén wave mode given by (A 16), and the other two are the fast and slow magnetoacoustic wave modes given by (A 17). In the following, these wave

https://doi.org/10.1017/S0022377818001228 Published online by Cambridge University Press

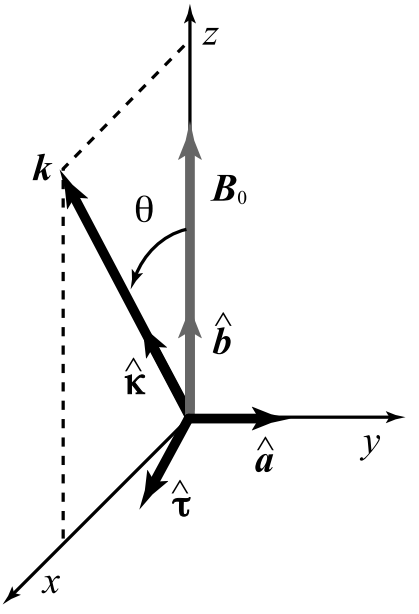

FIGURE 2. Magnetohydrodynamic wave configuration.

modes are argued in relation to the turbulent mass and internal-energy fluxes due to the dilatational cross-helicity effect.

In order to describe the eigenvector solutions of the velocity, magnetic-field and electric-field perturbations, $\delta\boldsymbol{u}$, $\delta\boldsymbol{b}$ and $\delta\boldsymbol{e}$, it is convenient to define a mutually orthogonal system of unit vectors. The unit vector in the direction of the mean magnetic field $\boldsymbol{B}$ is $\hat{\boldsymbol{b}}(=\boldsymbol{B}/|\boldsymbol{B}|)$. The unit vector along the wave vector is $\hat{\boldsymbol{\kappa}}(=\boldsymbol{k}/|\boldsymbol{k}|)$. In addition, $\hat{\boldsymbol{a}}$ and $\hat{\boldsymbol{\tau}}$ are the mutually orthogonal unit vectors to $\hat{\boldsymbol{\kappa}}$, which are defined by $\hat{\boldsymbol{a}} = -\boldsymbol{k}\times\boldsymbol{B}/|\boldsymbol{k}\times\boldsymbol{B}|$ and $\hat{\boldsymbol{\tau}} = \hat{\boldsymbol{a}}\times\hat{\boldsymbol{\kappa}}$. Without losing generality, we have $\boldsymbol{B}$ lie in the z direction and $\boldsymbol{k}$ vector in the z–x plane (figure 2). In this case, we have the unit vectors as

$$\hat{\boldsymbol{b}} = (0, 0, 1), \tag{5.13a}$$

$$\hat{\boldsymbol{\kappa}} = (\sin\theta, 0, \cos\theta), \tag{5.13b}$$

$$\hat{\boldsymbol{a}} = (0, 1, 0), \tag{5.13c}$$

$$\hat{\boldsymbol{\tau}} = (\cos\theta, 0, -\sin\theta). \tag{5.13d}$$

Transverse Alfvén mode

The transverse Alfvén mode given by (A 16) has eigenvectors

$$\delta\boldsymbol{u} \propto \delta\boldsymbol{b} \propto \hat{\boldsymbol{a}} = (0, 1, 0), \tag{5.14a}$$

$$\delta\boldsymbol{e} \propto \cos\theta\,\hat{\boldsymbol{\tau}} + \sin\theta\,\hat{\boldsymbol{\kappa}} = (1, 0, 0) \tag{5.14b}$$

(Cramer 2001). In the transverse Alfvén mode, velocity and magnetic-field perturbations are aligned with each other, and are in the direction perpendicular both to the mean magnetic field $\boldsymbol{B}$ and the wave vector $\boldsymbol{k}$. Both $\delta\boldsymbol{u}$ and $\delta\boldsymbol{b}$ are perpendicular to the wave vector $\hat{\boldsymbol{\kappa}}\cdot\delta\boldsymbol{u} = \hat{\boldsymbol{\kappa}}\cdot\delta\boldsymbol{b} = 0$. Since $\hat{\boldsymbol{\kappa}}\cdot\delta\boldsymbol{u} = 0$, we have no density variation $\delta\rho = 0$. The transverse Alfvén mode is purely incompressible.

https://doi.org/10.1017/S0022377818001228 Published online by Cambridge University Press

The group velocity of the transverse Alfvén mode is written as

$$\boldsymbol{v}_{\rm g} = \frac{\partial \omega}{\partial \boldsymbol{k}} = v_{\rm A} \cos\theta \hat{\boldsymbol{b}}, \tag{5.15}$$

where $v_{\rm A}$ is the Alfvén speed defined by (A 14). This implies that the material or mass is carried with this group velocity along the mean magnetic field $\boldsymbol{B}$ in the case of the transverse Alfvén mode.

The electric-field perturbation $\delta\boldsymbol{e}$ is not perpendicular to the wave vector ($\hat{\boldsymbol{\kappa}} \cdot \delta\boldsymbol{e} \neq 0$), but is perpendicular to the mean magnetic field ($\hat{\boldsymbol{b}} \cdot \delta\boldsymbol{e} = 0$). The Poynting flux due to the electric- and magnetic-field perturbations in the transverse Alfvén mode, $\boldsymbol{S}_{\rm A}$, is given by

$$\boldsymbol{S}_{\rm A} = \frac{\delta\boldsymbol{e} \times \delta\boldsymbol{b}}{\mu_0} \propto (\cos\theta \hat{\boldsymbol{\tau}} + \sin\theta \hat{\boldsymbol{\kappa}}) \times \hat{\boldsymbol{a}} = \cos\theta \hat{\boldsymbol{\kappa}} - \sin\theta \hat{\boldsymbol{\tau}} = (0, 0, 1) = \hat{\boldsymbol{b}}. \tag{5.16}$$

This shows that the wave energy is transferred along the mean magnetic field $\boldsymbol{B}$. This effect is a purely incompressible effect, so not directly related to the compressional cross-helicity effects $-\kappa_B \boldsymbol{B}$ or $-\eta_B \boldsymbol{B}$. However, as will be referred to in § 6, the solenoidal and dilatational parts of the cross-helicity are coupled with each other. If the transverse Alfvén waves provide solenoidal but highly aligned velocity and magnetic-field perturbations, the dilatational cross-helicity may be also generated at the nonlinear stage of compressible MHD flow, resulting in the compressional or dilatational cross-helicity effects in the turbulent mass and internal-energy transports.

Magnetoacoustic modes

The fast and slow magnetoacoustic modes given by (A 17) have eigenvectors

$$\delta\boldsymbol{u} \propto \cos\theta(\omega^2 - c_{\rm S}^2 k^2)\hat{\boldsymbol{\tau}} + \sin\theta\omega^2\hat{\boldsymbol{\kappa}} = (\omega^2 - c_{\rm S}^2 k^2 \cos^2\theta, 0, c_{\rm S}^2 k^2 \cos\theta \sin\theta), \tag{5.17a}$$

$$\delta\boldsymbol{b} \propto \hat{\boldsymbol{\tau}} = (\cos\theta, 0, -\sin\theta), \tag{5.17b}$$

$$\delta\boldsymbol{e} \propto \hat{\boldsymbol{a}} = (0, 1, 0) \tag{5.17c}$$

(Cramer 2001). Here, $c_{\rm S}$ is the sound speed defined by (A 15). In the magnetoacoustic modes, there are density perturbations ($\delta\rho \neq 0$) since $\boldsymbol{\nabla} \cdot \delta\boldsymbol{u} \neq 0$.

We see from (5.17*a*) and (5.17*b*) that the velocity perturbation $\delta\boldsymbol{u}$ has both perpendicular and parallel components to the wave vector $\boldsymbol{\kappa}$ while the magnetic perturbation is only in the direction perpendicular to $\hat{\boldsymbol{\kappa}}$ because of the solenoidal nature of $\delta\boldsymbol{b}$ ($\boldsymbol{\nabla} \cdot \delta\boldsymbol{b} = 0$). At the same time, there is a magnetic-field perturbation $\delta\boldsymbol{b}$, as well as a velocity perturbation $\delta\boldsymbol{u}$, that is parallel to the unperturbed magnetic field $\boldsymbol{B}$.

If we take the inner product of $\delta\boldsymbol{u}$ (5.17*a*) and $\delta\boldsymbol{b}$ (5.17*b*) in the magnetoacoustic modes, we get

$$\delta\boldsymbol{u} \cdot \delta\boldsymbol{b} \propto [\cos\theta(\omega^2 - c_{\rm S}^2 k^2)\hat{\boldsymbol{\tau}} + \sin\theta\omega^2\hat{\boldsymbol{\kappa}}] \cdot \hat{\boldsymbol{\tau}} = \cos\theta(\omega^2 - c_{\rm S}^2 k^2). \tag{5.18}$$

Since the magnetic perturbation $\delta\boldsymbol{b}$ has no components in the $\boldsymbol{\kappa}$ direction (5.17*b*), the cross-helicity due to the velocity and magnetic-field perturbations (turbulent cross-helicity) is generated only by the combination of the velocity and magnetic-field perturbations transverse to the wave vector $\boldsymbol{k}$. The sign of the turbulent cross-helicity depends on the angle θ between the wave propagation $\boldsymbol{k}$ and the mean magnetic field $\boldsymbol{B}$. The magnitude of the turbulent cross-helicity is expected to be maximum when the wave propagation is parallel or antiparallel to $\boldsymbol{B}$ ($\theta = 0$ or π). Also even

https://doi.org/10.1017/S0022377818001228 Published online by Cambridge University Press

in the case of $\theta = 0$ or π, if the phase velocity is represented by the sound speed: $u_\phi = c_S$ or equivalently $\omega^2 = c_S^2 k^2$, the velocity perturbation along $\boldsymbol{\tau}$ vanishes, then the velocity perturbation $\delta\boldsymbol{u}$ and the magnetic-field perturbation $\delta\boldsymbol{b}$ are orthogonal to each other. In this case, we have no turbulent cross-helicity. This is the case of the slow mode: the electromagnetic component completely disappears at $\theta = 0$, π and the slow mode wave is reduced to a sound wave. On the other hand, if the wave propagation direction is perpendicular to the unperturbed magnetic field ($\theta = \pi/2$), the velocity and magnetic perturbation are orthogonal to each other, then we have no turbulent cross-helicity. This is the case for the magnetoacoustic wave propagating in the perpendicular direction to $\boldsymbol{B}$.

The Poynting flux due to the electric- and magnetic-field perturbations in the magnetoacoustic modes, $\boldsymbol{S}_M$, is given by

$$\boldsymbol{S}_M = \frac{\delta\boldsymbol{e} \times \delta\boldsymbol{b}}{\mu_0} \propto \hat{\boldsymbol{a}} \times \hat{\boldsymbol{\tau}} = \hat{\boldsymbol{a}} \times (\hat{\boldsymbol{a}} \times \hat{\boldsymbol{\kappa}}) = -\hat{\boldsymbol{a}}^2 \hat{\boldsymbol{\kappa}} = -\hat{\boldsymbol{\kappa}}. \tag{5.19}$$

This shows that the wave energy is transferred along the wave vector in the direction opposite to $\boldsymbol{k}$ or $\boldsymbol{\kappa}(\equiv \boldsymbol{k}/|\boldsymbol{k}|)$.

These arguments suggest that the magnetoacoustic modes are, to some extent, the linearised counterpart of the compressive cross-helicity effect we obtained in §§ 4 and 5.1, since these modes have both compressibility and cross-helicity simultaneously. At the same time, the transverse Alfvén mode is very important for providing the turbulent cross-helicity. We should note that the cross-helicity is constituted only of the solenoidal motion and magnetic field both in the transverse Alfvén and magnetoacoustic modes as (5.14*a*), (5.17*a*), (5.17*b*) and (5.18) show.

In the linearised MHD wave argument, mass and energy are considered to be carried in the direction of the mean magnetic field (transverse Alfvén mode) and in the direction to the wave vector (magnetoacoustic modes). Deviation from the aligned transport, i.e. a transfer in the direction oblique to $\boldsymbol{B}$ or $\boldsymbol{k}$, may require some nonlinear, resistive or kinetic effects. On the other hand, in the arguments with strongly turbulent or nonlinear MHD processes, the gradient diffusion should be the effect of primary importance, and deviations from the gradient diffusion in the turbulent mass and energy transports show up with the strong density-variance effects in cross-diffusion and the compressional cross-helicity effects in transport along the mean magnetic field.

Both these effects need compressibility and the aligned components of the velocity and magnetic-field perturbations. However, there are several differences between these two effects. For example, as with the physical interpretation given in § 5.1, the compressive cross-helicity effect requires the inhomogeneity of the magnetic fluctuations along the mean magnetic field. In the magnetoacoustic modes, such magnetic fluctuation is not allowed to exist if the wave propagation is along the unperturbed magnetic field ($\theta = 0$, π) (see (5.17*b*)).

6. Summary and concluding remarks

Summary

In this work, strongly compressible MHD turbulence was analysed with the aid of the multiple-scale direct-interaction approximation (multiple-scale DIA), an analytical closure scheme for inhomogeneous turbulence at very high Reynolds numbers. The theoretical expressions for the turbulent mass flux $\langle \rho' \boldsymbol{u}' \rangle$ (4.16) and the turbulent

https://doi.org/10.1017/S0022377818001228 Published online by Cambridge University Press

internal-energy flux $\langle q' \boldsymbol{u}' \rangle$ (4.28) are obtained with the analytical expressions of the transport coefficients (4.17)–(4.20) and (4.29)–(4.31), respectively, in terms of the Green's and spectral functions of turbulence. Using the analytical results, a turbulence model with one-point turbulent quantities and the time scales of turbulence was proposed as (4.33)–(4.39). In addition to the usual gradient-diffusion model, the cross-diffusion mediated by the density variance $\langle \rho'^2 \rangle$ and the transfer along the mean magnetic field mediated by the compressional cross-helicity effect are obtained, and suggested to be included in the expression for the turbulent mass and internal-energy fluxes, $\langle \rho' \boldsymbol{u}' \rangle$ and $\langle q' \boldsymbol{u}' \rangle$. These effects can be important in providing deviations from the gradient-diffusion fluxes. The relationship of the compressional cross-helicity effect with the magnetoacoustic waves was also argued.

Concluding remarks

As the model expressions for the turbulence transport coefficients (4.33)–(4.39) show, the spatio-temporal evolutions of the density variance $\langle \rho'^2 \rangle$ and the turbulent cross-helicity $\langle \boldsymbol{u}' \cdot \boldsymbol{b}' \rangle$ are of crucial importance for the evaluation of effects other than the gradient diffusion, namely, the cross-diffusion and transport along the mean magnetic field. As for the evolution equation of $\langle \rho'^2 \rangle$, this was already discussed in Paper 1 (Yokoi 2018) in the context of the turbulent electromotive force in strongly compressible MHD turbulence (e.g. § 5 of Paper 1). Here, we note the evolution of the turbulent cross-helicity.

The conservative property of the global cross-helicity integral $\int_V \boldsymbol{u} \cdot \boldsymbol{b} \, \mathrm{d}V$ has been argued for a long time (Woltjer 1958). This invariance nature yields a topological interpretation of the cross-helicity. The global integral of the cross-helicity is a measure of the linkage of the vortex lines with the magnetic-field lines (Moffatt 1978). However, as compared with the arguments for the magnetic helicity and also for the kinetic helicity, the counterparts for the cross-helicity have been limited.

It is well known that the presence of the turbulent cross-helicity $\langle \boldsymbol{u}' \cdot \boldsymbol{b}' \rangle$ is closely related to the asymmetry of the Alfvén wave propagation between the directions parallel and antiparallel to the large-scale magnetic field (Yokoi 2013). Actually, this asymmetry of the Alfvén wave propagation is the main source of the very high amplitudes of the turbulent cross-helicity in solar-wind turbulence (Tu & Marsch 1995; Bruno & Carbone 2016). At the same time, there are several other sources of turbulent cross-helicity in inhomogeneous MHD turbulence. Inhomogeneities of the mean-field structures such as the mean magnetic-field strain and the large-scale vortical motion coupled with the turbulent correlations (the Reynolds stress, the turbulent Maxwell stress, the turbulent electromotive force, etc.) provide the production mechanisms of the turbulent cross-helicity other than the asymmetry of the Alfvén wave propagation (Yokoi 2011; Yokoi & Hoshino 2011). In this sense, the turbulent cross-helicity represents broader contents than just an asymmetry of the Alfvén wave propagation.

In the compressible MHD turbulence case, we have additional production mechanisms intrinsic to the compressibility. The evolution equation of the local density of the turbulent cross-helicity $\langle \boldsymbol{u}' \cdot \boldsymbol{b}' \rangle$ in the compressible MHD case is written as (Yokoi 2013)

$$\begin{aligned} \frac{\mathrm{D}}{\mathrm{D}t} \langle \boldsymbol{u}' \cdot \boldsymbol{b}' \rangle \;=\; & -\frac{1}{2} \left\langle u'^a u'^b - \frac{1}{\mu_0 \overline{\rho}} b'^a b'^b \right\rangle \left(\frac{\partial B^b}{\partial x^a} + \frac{\partial B^a}{\partial x^b} \right) - \langle \boldsymbol{u}' \times \boldsymbol{b}' \rangle \cdot \boldsymbol{\Omega} \\ & - (\gamma_s - 1) \frac{1}{\overline{\rho}} \langle \rho' \boldsymbol{b}' \rangle \cdot \nabla Q - (\gamma_s - 1) \frac{1}{\overline{\rho}} \langle q' \boldsymbol{b}' \rangle \cdot \nabla \overline{\rho} - \frac{1}{\overline{\rho}} \langle \rho' \boldsymbol{b}' \rangle \cdot \frac{\mathrm{D}\boldsymbol{U}}{\mathrm{D}t} \\ & - \langle \boldsymbol{u}' \cdot \boldsymbol{b}' \rangle \nabla \cdot \boldsymbol{U} + \boldsymbol{B} \cdot \nabla \left\langle \frac{1}{2} \boldsymbol{u}'^2 \right\rangle - \varepsilon_W + T_W + \mathrm{R.T.}, \end{aligned} \tag{6.1}$$

https://doi.org/10.1017/S0022377818001228 Published online by Cambridge University Press

where R.T. denotes the residual terms, and ε_W and T_W are respectively the dissipation and transport rates of the turbulent cross-helicity, whose detailed expressions are suppressed here. We see from (6.1) how and under what conditions the turbulent cross-helicity and its compressive part can be generated. For instance, the asymmetry between the parallel and antiparallel propagations of the Alfvén waves along the mean magnetic field $\boldsymbol{B}$ is related to the second term of the final line, or the $\boldsymbol{B}\cdot\nabla\langle\boldsymbol{u}'^2\rangle/2$ term in (6.1). Inhomogeneity along the mean magnetic field in general provides a source of non-zero or finite turbulent cross-helicity. Another important point is that (6.1) has genuine compressible production terms. The ∇Q-, $\nabla\overline{\rho}$-, and $D\boldsymbol{U}/Dt$-related terms on the second line in (6.1) are such compressibility-originated terms. These terms, as well as the $\nabla\cdot\boldsymbol{U}$ or mean dilatation term, give the possibility to generate turbulent cross-helicity even in the absence of the mean magnetic field $\boldsymbol{B}$. In this sense, as compared with the solenoidal MHD turbulence, strongly compressible MHD turbulence provides us with interesting situations where the cross-helicity plays an important role in turbulent transport.

Validation of the present theoretical results and the turbulence model based on them can be numerically performed. An extension of Kolmogorov flow with an imposed uniform magnetic field in the inhomogeneous direction (Yokoi & Balarac 2011) to a compressible case is one possible set-up for the numerical validation. Another more artificial set-up may be an MHD counterpart of the global flow generation (Yokoi & Brandenburg 2016). In the latter case, the turbulent cross-helicity is externally injected by forcing, and the coupling of this turbulent cross-helicity with an externally imposed uniform magnetic field should be examined in the context of the turbulent mass and internal-energy fluxes. As referred to in § 1, the amount of compressible turbulence forcing is expected to be a key parameter determining the star formation rate in molecular clouds. These numerical experiments in the context of the present effects are left for future interesting works.

Acknowledgements

Part of this work was conducted under the support of the JSPS Grants-in-Aid for Scientific Research 18H01212 and that of the ISEE (Nagoya University) Collaborative Research Program 2017. Part of this work was performed during the author's stay at Consorzio RFX in Padova (hosted by S. Cappello) and the Max-Planck Institut für Sonnensystemforschung (MPS) in Göttingen (by M. Käpylä) in September 2018 as a visiting researcher. His thanks are also due to anonymous referees for their constructive comments for improving the presentation of the paper.

Appendix A. Dispersive relation of magnetohydrodynamic waves

Following standard textbooks (Cross 1988; Cramer 2001; Gurnett & Bhattacharjee 2017), we present a way to derive the dispersion relation of the magnetohydrodynamic waves.

We consider small disturbances for the field quantities as $\rho=\overline{\rho}+\rho'$, $\boldsymbol{u}=\boldsymbol{U}+\boldsymbol{u}'=\boldsymbol{u}'$, $\boldsymbol{b}=\boldsymbol{B}+\boldsymbol{b}'$, $p=P+p'$. Assuming that the disturbances are small, we linearise the ideal magnetohydrodynamic equations for the perturbations. If the unperturbed system is uniform and static, we introduce the Fourier representation of the perturbed quantities as

$$f'(\boldsymbol{x};t)=\hat{f}(k;\omega)\exp\left[\mathrm{i}(\boldsymbol{k}\cdot\boldsymbol{x}-\omega t)\right]. \tag{A 1}$$

https://doi.org/10.1017/S0022377818001228 Published online by Cambridge University Press

With (A 1), the differential operators are transformed as $\nabla \to \mathrm{i}\boldsymbol{k}$ and $\partial/\partial t \to -\mathrm{i}\omega$. Then, the equations of the perturbations are written as

$$-\mathrm{i}\omega\hat{\rho}' + \mathrm{i}\overline{\rho}\,\boldsymbol{k}\cdot\hat{\boldsymbol{u}}' = 0, \tag{A 2}$$

$$-\mathrm{i}\omega\overline{\rho}\,\hat{\boldsymbol{u}}' = \frac{\mathrm{i}}{\mu_0}(\boldsymbol{k}\times\hat{\boldsymbol{b}}')\times\boldsymbol{B} - \mathrm{i}\boldsymbol{k}\,\hat{p}', \tag{A 3}$$

$$-\mathrm{i}\omega\hat{\boldsymbol{b}}' = \mathrm{i}\boldsymbol{k}\times(\hat{\boldsymbol{u}}'\times\boldsymbol{B}), \tag{A 4}$$

$$\mathrm{i}\boldsymbol{k}\cdot\hat{\boldsymbol{b}}' = 0, \tag{A 5}$$

$$\hat{p}' = c_{\mathrm{S}}^2\hat{\rho}', \tag{A 6}$$

where c_{S} is the speed of sound defined by $c_{\mathrm{S}}^2 = \partial\hat{p}/\partial\hat{\rho} = \gamma_{\mathrm{s}}P/\overline{\rho}$. At this point we drop the hat from $\hat{f}'$ for the perturbed quantities in the wavenumber space, and write simply f'.

Eliminating p' from (A 6) with (A 2), we have equation of $\boldsymbol{u}'$ as

$$\omega^2\boldsymbol{u}' = \frac{1}{\mu_0\overline{\rho}}\{\boldsymbol{k}\times[\boldsymbol{k}\times(\boldsymbol{u}'\times\boldsymbol{B})]\}\times\boldsymbol{B} + c_{\mathrm{S}}^2\boldsymbol{k}(\boldsymbol{k}\cdot\boldsymbol{u}'). \tag{A 7}$$

Here, we have used (A 4) for eliminating $\boldsymbol{b}'$.

Without losing generality, we can put the unperturbed magnetic field $\boldsymbol{B}$ and the wave vector $\boldsymbol{k}$ as

$$\boldsymbol{B} = (0, 0, B_0), \tag{A 8}$$

$$\boldsymbol{k} = (k\sin\theta, 0, k\cos\theta). \tag{A 9}$$

We also introduce the phase velocity $u_\phi(=\sqrt{\omega^2/k^2})$ and the Alfvén speed $v_{\mathrm{A}}(=\sqrt{\boldsymbol{B}^2}/\sqrt{\mu_0\overline{\rho}})$. From the induction equation (A 4) or equivalently

$$\begin{pmatrix} b'^x \\ b'^y \\ b'^z \end{pmatrix} = \begin{pmatrix} -(B/u_\phi)\cos\theta & 0 & 0 \\ 0 & -(B/u_\phi)\cos\theta & 0 \\ (B/u_\phi)\sin\theta & 0 & 0 \end{pmatrix} \begin{pmatrix} u'^x \\ u'^y \\ u'^z \end{pmatrix}. \tag{A 10}$$

This shows that the perturbed velocity $\boldsymbol{u}'$ along the unperturbed magnetic field $\boldsymbol{B}$, u'^z, does not contribute to the magnetic-field perturbation $\boldsymbol{b}'$ at all.

From the momentum equation (A 7), we have

$$\begin{pmatrix} u_\phi^2 - c_{\mathrm{S}}^2\sin^2\theta - v_{\mathrm{A}}^2 & 0 & -c_{\mathrm{S}}^2\sin\theta\cos\theta \\ 0 & u_\phi^2 - v_{\mathrm{A}}^2\cos^2\theta & 0 \\ -c_{\mathrm{S}}^2\sin\theta\cos\theta & 0 & u_\phi^2 - c_{\mathrm{S}}^2\cos^2\theta \end{pmatrix} \begin{pmatrix} u'^x \\ u'^y \\ u'^z \end{pmatrix} = \boldsymbol{0}. \tag{A 11}$$

Note that there is no coupling between the equation involving u'^y and the equations involving u'^x and u'^z.

This equation has non-trivial solutions for $\boldsymbol{u}'$ only if the determinant of the matrix is zero. This gives the dispersion relation:

$$(u_\phi^2 - v_{\mathrm{A}}^2\cos^2\theta)[u_\phi^4 - (v_{\mathrm{A}}^2 + c_{\mathrm{S}}^2)u_\phi^2 + v_{\mathrm{A}}^2c_{\mathrm{S}}^2\cos^2\theta] = 0, \tag{A 12}$$

where θ is the angle between the unperturbed magnetic field $\boldsymbol{B}$ and the wave vector $\boldsymbol{k}$ ($k = |\boldsymbol{k}|$) (Cross 1988; Cramer 2001; Gurnett & Bhattacharjee 2017). Here u_ϕ is the phase velocity, v_{A} is the Alfvén speed and c_{S} is the speed of sound defined by

$$u_\phi^2 = \omega^2/k^2, \tag{A 13}$$

https://doi.org/10.1017/S0022377818001228 Published online by Cambridge University Press

$$v_{\mathrm{A}}^2 = \boldsymbol{B}^2/(\mu_0\overline{\rho}), \tag{A 14}$$

$$c_{\mathrm{S}}^2 = \gamma_{\mathrm{s}} p/\rho, \tag{A 15}$$

respectively.

The dispersion relation (A 12) has three roots. One is the transverse or shear Alfvén mode given by

$$u_\phi^2 = v_{\mathrm{A}}^2 \cos^2\theta. \tag{A 16}$$

The remaining other two are the fast and slow magnetoacoustic modes given by

$$u_\phi^2 = \tfrac{1}{2}(v_{\mathrm{A}}^2 + c_{\mathrm{S}}^2) \pm \tfrac{1}{2}[(v_{\mathrm{A}}^2 - c_{\mathrm{S}}^2)^2 + 4v_{\mathrm{A}}^2 c_{\mathrm{S}}^2 \cos^2\theta]^{1/2}, \tag{A 17}$$

where the plus and minus signs in the double signs correspond to the fast and slow modes, respectively.

REFERENCES

ALUIE, H. 2011 Compressible turbulence: the cascade and its locality. *Phys. Rev. Lett.* **106**, 174502.

BATCHELOR, G. K. 1953 *The Theory of Homogeneous Turbulence*. Cambridge University Press.

BRAGINSKY, S. & ROBERTS, P. 1995 Equations governing convection in Earth's core and the geodynamo. *Geophys. Astrophys. Fluid Dyn.* **79**, 1–97.

BRUNO, R. & CARBONE, V. 2016 *Turbulence in the Solar Wind*. Springer.

CHASSAING, P., ANTONIA, R. A., ANSELMET, F., JOLY, L. & SARKAR, S. 2002 *Variable Density Fluid Turbulence*. Kluwer.

CRAMER, N. F. 2001 *The Physics of Alfvén Waves*. Wiley-VCH.

CROSS, R. 1988 *An Introduction to Alfven Waves*. Adam Hilger.

FEDERRATH, C. & KLESSEN, R. S. 2012 The star formation rate of turbulent magnetized clouds: comparing theory, simulations, and observations. *Astrophys. J.* **761**, 156.

GURNETT, D. & BHATTACHARJEE, A. 2017 *Introduction to Plasma Physics: With Space, Laboratory and Astrophysical Applications*, 2nd edn. Cambridge University Press.

HAMBA, F. 1987 Statistical analysis of chemically reacting passive scalars in turbulent shear flow. *J. Phys. Soc. Japan* **56**, 79–96.

HIGASHIMORI, K., YOKOI, N. & HOSHINO, M. 2013 Explosive turbulent magnetic reconnection. *Phys. Rev. Lett.* **110**, 255001.

HINZE, J. O. 1975 *Turbulence*, 2nd edn. Springer.

KAVIANY, M. 2001 *Principles of Convective Heat Transfer*, 2nd edn. Springer.

KRAICHNAN, R. 1959 The structure of isotropic turbulence at very high Reynolds number. *J. Fluid Mech.* **5**, 497–543.

KRAUSE, F. & RÄDLER, K.-H. 1980 *Mean-Field Magnetohydrodynamics and Dynamo Theory*. Pergamon.

KRITSUK, A., USTYUGOV, S. D. & NORMAN, M. L. 2017 The structure and statistics of interstellar turbulence. *New J. Phys.* **19**, 065003.

KUPKA, F. 2009 Turbulent convection and numerical simulations in solar and stellar astrophysics. In *Interdisciplinary Aspects of Turbulence* (ed. W. Hillebrandt & F. Kupka), Lecture Notes in Physics, vol. 756, pp. 49–105. Springer.

LESIEURE, M. 2008 *Turbulence in Fluids: Fourth Revised and Enlarged Edition*. Springer.

LINDEN, P. F. 2000 Convection in the environment. In *Perspectives in Fluid Dynamics: A Collective Introduction to Current Research* (ed. G. K. Batchelor, H. K. Moffatt & M. G. Worster), pp. 289–345. Cambridge University Press.

MABANTA, Q. A. & MURPHY, J. W. 2018 How turbulence enables core-collapse supernova explosion. *Astrophys. J.* **856**, 22-1-14.

MAC LOW, M.-M. & KLESSEN, R. S. 2004 Control of star formation by supersonic turbulence. *Rev. Mod. Phys.* **76**, 125–194.

https://doi.org/10.1017/S0022377818001228 Published online by Cambridge University Press

McKee, C. F. & Ostriker, E. C. 2007 Theory of star formation. *Annu. Rev. Astron. Astrophys.* **45**, 565–687.

Meakin, C. & Arnett, W. D. 2010 Some properties of the kinetic energy flux and dissipation in turbulent stellar convection zones. *Astrophys. Space Sci.* **328**, 221–225.

Mihalas, D. & Weibel-Mihalas, B. 1984 *Foundations of Radiation Hydrodynamics*. Oxford University Press.

Moffatt, H. K. 1978 *Magnetic Field Generation in Electrically Conducting Fluids*. Cambridge University Press.

Murphy, J. W. & Meakin, C. 2011 A global turbulence model for neutrino-driven convection in core-collapse supernovae. *Astrophys. J.* **742**, 74-1-21.

Parker, E. N. 1955 Hydromagnetic dynamo models. *Astrophys. J.* **122**, 293–314.

Rogachevskii, I. & Kleeorin, N. 2015 Turbulent fluxes of entropy and internal energy in temperature stratified flows. *J. Plasma Phys.* **81**, 395810504.

Tennekes, H. & Lumley, J. L. 1972 *A First Course in Turbulence in Turbulence*. MIT Press.

Tu, C.-Y. & Marsch, E. 1995 *MHD Structures, Waves and Turbulence in the Solar Wind: Observations and Theories*. Kluwer.

Turner, J. S. 1973 *Buoyancy Effects in Fluids*. Cambridge University Press.

Widmer, F., Büchner, J. & Yokoi, N. 2016 Sub-grid-scale description of turbulent magnetic reconnection in magnetohydrodynamics. *Phys. Plasmas* **23**, 042311.

Widmer, F., Büchner, J. & Yokoi, N. 2016 Characterizing plasmoid reconnection by turbulence dynamics. *Phys. Plasmas* **23**, 092304.

Woltjer, L. 1958 A theorem on force-free magnetic fields. *Proc. Natl Acad. Sci. USA* **44**, 489–491.

Yokoi, N. 2011 Modeling the turbulent cross-helicity evolution: production, dissipation, and transport rates. *J. Turbul.* **12**, N27-1-33.

Yokoi, N. 2013 Cross helicity and related dynamo. *Geophys. Astrophys. Fluid Dyn.* **107**, 114–184.

Yokoi, N. 2018 Electromotive force in strongly compressible magnetohydrodynamic turbulence. *J. Plasma Phys.* **84**, 735840501.

Yokoi, N. & Balarac, G. 2011 Cross-helicity effects and turbulent transport in magnetohydrodynamic flow. *J. Phys. Conf. Ser.* **318**, 072039.

Yokoi, N. & Brandenburg, A. 2016 Large-scale flow generation by inhomogeneous helicity. *Phys. Rev.* E **93**, 033125.

Yokoi, N. & Hoshino, M. 2011 Flow–turbulence interaction in magnetic reconnection. *Phys. Plasmas* **18**, 111208.

Yokoi, N. & Yoshizawa, A. 1993 Statistical analysis of the effects of helicity in inhomogeneous turbulence. *Phys. Fluids* A **5**, 464–477.

Yokoi, N., Higashimori, K. & Hoshino, M. 2013 Transport enhancement and suppression in turbulent magnetic reconnection: a self-consistent turbulence model. *Phys. Plasmas* **20**, 122310.

Yoshizawa, A. 1984 Statistical analysis of the deviation of the Reynolds stress from its eddy-viscosity representation. *Phys. Fluids* **27**, 1377–1387.

Yoshizawa, A. 1990 Self-consistent turbulent dynamo modeling of reversed field pinches and planetary magnetic fields. *Phys. Fluids* B **2**, 1589–1600.

Yoshizawa, A. 1996 Compressibility and rotation effects on transport suppression in magnetohydrodynamic turbulence. *Phys. Plasmas* **3**, 889–900.

Yoshizawa, A. & Yokoi, N. 1993 Turbulent magnetohydrodynamic dynamo for accretion disks using the cross-helicity effect. *Astrophys. J.* **407**, 540–548.